

---

# Strong Screening Rules for Group-based SLOPE Models

---

**Fabio Feser**

Department of Mathematics  
Imperial College London  
London, SW7 2AZ  
ff1200ic.ac.uk

**Marina Evangelou**

Department of Mathematics  
Imperial College London  
London, SW7 2AZ  
m.evangelou@ic.ac.uk

## Abstract

Tuning the regularization parameter in penalized regression models is an expensive task, requiring multiple models to be fit along a path of parameters. Strong screening rules drastically reduce computational costs by lowering the dimensionality of the input prior to fitting. We develop strong screening rules for group-based Sorted L-One Penalized Estimation (SLOPE) models: Group SLOPE and Sparse-group SLOPE. The developed rules are applicable for the wider family of group-based OWL models, including OSCAR. Our experiments on both synthetic and real data show that the screening rules significantly accelerate the fitting process. The screening rules make it accessible for group SLOPE and sparse-group SLOPE to be applied to high-dimensional datasets, particularly those encountered in genetics.

## 1 Introduction

As the amount of data collected increases, the emergence of high-dimensional data, where the number of features ( $p$ ) is much larger than the number of observations ( $n$ ), is becoming increasingly common in fields ranging from genetics to finance. Performing regression and discovering relevant features on these datasets is a challenging task, as classical statistical methods tend to break down. The most popular approach to meeting this challenge is the *Lasso* [30], which has given rise to the general penalized regression framework

$$\hat{\beta}(\lambda) = \arg \min_{\beta \in \mathbb{R}^p} \{f(\beta) + \lambda J(\beta; v)\}, \quad (1)$$

where  $f$  is the loss function,  $J$  is a convex penalty norm,  $v \succeq 0$  are penalty parameters, and  $\lambda > 0$  is the regularization parameter.

A key aspect of fitting a penalized model is to tune the value of the regularization parameter, which determines the level of sparsity in the fitted model. Several approaches exist for tuning this parameter, including cross-validation [8, 15] and exact solution path algorithms [10], but can often be computationally expensive. Generally, the model is fit along an  $l$ -length path  $\lambda_1 \geq \dots \geq \lambda_l \geq 0$ . Finding approaches for speeding up the model fitting process can lead to large computational savings when tuning. Screening rules are popular methods that reduce the dimensions of the input dimensionality by discarding irrelevant features before the fitting process. Discarding features, especially in high-dimensional settings, has a tremendous impact on the computational costs.

Denoting the *active set* of non-zero parameters at  $\lambda_{k+1}$  by  $\mathcal{A}_v(\lambda_{k+1}) = \{i \in \{1, \dots, p\} : \hat{\beta}_i(\lambda_{k+1}) \neq 0\}$ , the goal of a screening rule is to use the solution at  $\lambda_k$  to recover a *screened set* of features,  $\mathcal{S}_v(\lambda_{k+1})$ , which is a superset of  $\mathcal{A}_v(\lambda_{k+1})$ . The screened set can then be used as input for calculating the fitted values. By finding the smallest possible screened set, that still contains the active set, the number of irrelevant features included in the optimization process is reduced.

There are two types of screening rules: *safe* and *heuristic*. Safe rules, as suggested by the name, provide guarantees that any variables discarded are in fact inactive at the solution. The seminal work of El Ghaoui et al. [11] introduced the Safe Feature Elimination Rule (SAFE) for the lasso, in which safe regions were constructed to eliminate non-active features. Other examples of safe rules are given in [2, 25, 34], including sample screening [28]. Heuristic rules, on the other hand, tend to discard more variables, but this increased screening efficiency can lead to active variables being incorrectly discarded. Examples of heuristic screening rules are given in [1, 13, 31]. Amongst the proposed heuristic rules, of particular interest is the strong screening rule framework developed for the lasso [31]. As strong screening rules can lead to violations, Tibshirani et al. [31] complemented their rules with a check of the Karush–Kuhn–Tucker (KKT) [16] optimality conditions to ensure no violations occur. There are also hybrid screening regimes, which combine safe and heuristic rules [32, 37].

A strong screening rule is formulated through the KKT conditions for Equation 1, given by:

$$\mathbf{0} \in \nabla f(\beta) + \lambda \partial J(\beta; v). \quad (2)$$

If the gradient  $\nabla f(\hat{\beta}(\lambda_{k+1}))$  was available, the set  $\mathcal{A}_v(\lambda_{k+1})$  could be identified by checking the subdifferential of the norm at zero. That is, identifying for which variables

$$-\nabla f(\beta) \in \lambda \partial J(\mathbf{0}; v) = \{x \in \mathbb{R}^p : J^*(x; \lambda v) \leq 1\}, \quad (3)$$

where  $J^*$  refers to the dual norm of  $J$ . The subdifferential at zero,  $\partial J(\mathbf{0}; v)$ , can also be seen to be the unit ball of its dual norm. As the gradient at  $\lambda_{k+1}$  is not available in practice, an approximation of the gradient is used to find a screened subset of the features,  $\mathcal{S}_v(\lambda_{k+1})$ . The screened variables are combined with the previously active ones to form the reduced input space,  $\mathcal{E}_v(\lambda_{k+1}) = \mathcal{S}_v(\lambda_{k+1}) \cup \mathcal{A}_v(\lambda_k)$ . The fitted values are then calculated by solving Equation 1 using only the variables in  $\mathcal{E}_v(\lambda_{k+1})$ . Optimality of the fitted values is checked for using the KKT conditions (Equation 2), with violations added into  $\mathcal{E}_v$ . This ensures features are not discarded that should be active.

## 1.1 Contributions

Over the years, several adaptive extensions to the lasso have been proposed, including the *Sorted L-One Penalized Estimation (SLOPE)* method [4]. SLOPE applies the sorted  $\ell_1$  norm  $J_{\text{slope}}(\beta; v) = \sum_{i=1}^p v_i |\beta|_{(i)}$ , where  $v_1 \geq \dots \geq v_p \geq 0$ ,  $|\beta|_{(1)} \geq \dots \geq |\beta|_{(p)}$ . One key advantage of SLOPE is its ability to control the variable false discovery rate (FDR) under orthogonal data. Both safe and strong rules have been proposed for SLOPE [3, 12, 17], as well as exact solution path algorithms [9, 24]. As SLOPE is a non-separable penalty, safe screening rules require repeated screening during the fitting process [17]. This can be a computational bottleneck, as the calculation of the safe regions required for screening are often expensive.

Strong screening rules, on the other hand, are usually more time efficient as the extra cost of the screening and KKT checks tend to be outweighed by the significant savings of fitting on a reduced input space [31]. Motivated by this, we introduce strong screening rules for two group-based extensions of SLOPE: *Group SLOPE (gSLOPE)* [6] and *Sparse-group SLOPE (SGS)* [14].

Group SLOPE (gSLOPE) is an extension of SLOPE for selecting groups, defined by the norm

$$J_{\text{gslope}}(\beta; w) = \sum_{g=1}^m \sqrt{p_g} w_g \|\beta^{(g)}\|_2, \quad (4)$$

such that  $\beta^{(g)} \in \mathbb{R}^{p_g}$  is a vector of the group coefficients and  $p_g$  denotes the group sizes [6]. The norm has ordered penalty weights  $w_1 \geq \dots \geq w_m \geq 0$  (described in Appendix A.1) which are matched to  $\sqrt{p_1} \|\beta^{(1)}\|_2 \geq \dots \geq \sqrt{p_m} \|\beta^{(m)}\|_2$ .

Sparse-group SLOPE (SGS) was proposed as an extension to SLOPE and gSLOPE, applying both variable and group penalization for bi-level selection [14]. For  $\alpha \in [0, 1]$  with variable weights  $v$  and group weights  $w$  (described in Appendix B.1), the SGS norm is defined as

$$J_{\text{sgs}}(\beta; \alpha, v, w) = \alpha J_{\text{slope}}(\beta; v) + (1 - \alpha) J_{\text{gslope}}(\beta; w).$$

Both of these approaches were developed for the analysis of features that naturally belong to groups. This situation is frequently encountered in the analysis of genetics data, where genes are grouped into pathways for the completion of a specific biological task. The gSLOPE approach selects groups

of features, whereas SGS performs bi-level selection. Both approaches have been shown to inherit SLOPE’s ability to control FDR under orthogonal data: gSLOPE controls the group FDR [6] and SGS controls both variable and group FDRs [14].

Section 2 introduces a sparse-group screening rule framework. Based on this, strong screening rules for gSLOPE and SGS are developed and presented in Sections 3 and 4. The proofs of the theorems and propositions presented in Sections 2 and 3 are provided in the Appendices A.2 and B.3. Through a series of simulations and the analysis of real datasets (Sections 5), the proposed screening rules are shown to significantly reduce computational runtime. Additionally, due to the reduced input dimensionality offered by screening rules, issues with convergence in the analysis of large datasets are shown to be alleviated. These improvements are achieved without affecting the solution optimality.

The screening rules proposed in this manuscript are further applicable to group-based Ordered Weighted  $\ell_1$  (OWL) models. SLOPE is a particular case of an OWL model through the definition of its weights. As the proposed screening rules only require that the penalty sequences  $(v, w)$  are ordered, they can be used for any group-based OWL models; for example, the Octagonal Shrinkage and Clustering Algorithm for Regression (OSCAR) model [5]. Results for group-based OSCAR models are provided in Appendix E.

**Notation.** The feature space is divided into a set of  $m$  non-overlapping groups, where  $\mathcal{G}_1, \dots, \mathcal{G}_m$  denote the set of variable indices for each group. The set of active groups is denoted by  $\mathcal{A}_g = \{i \in \{1, \dots, m\} : \|\hat{\beta}^{(i)}\|_2 \neq 0\}$  whereas  $\mathcal{Z} = \{i \in \{1, \dots, m\} : \|\hat{\beta}^{(i)}\|_2 = 0\}$  presents the inactive groups. The set of variable indices of the active and inactive groups are denoted by  $\mathcal{G}_{\mathcal{A}}$  and  $\mathcal{G}_{\mathcal{Z}}$ , respectively. The cardinality of a vector  $x$  is denoted by  $\text{card}(x)$ . The operators  $(\cdot)_\downarrow$  and  $(\cdot)_{|\downarrow|}$  sort a vector into decreasing and decreasing absolute form. We use  $\preceq$  to denote element-wise less than or equal to. The operator  $\mathcal{O}(\cdot)$  returns the index of a vector sorted in decreasing absolute form. The cumulative summation operator applied on a vector is denoted by  $\text{cumsum}(x) = [x_1, x_1 + x_2, \dots, \sum_{i=1}^{\text{card}(x)} x_i]$ .

## 2 Screening rule framework

Sparse-group models apply both variable and group penalization, such that Equation 1 is extended to include an additional convex penalty function. Examples of sparse-group models include the Sparse-group Lasso (SGL) [29] and SGS [14]. Safe screening rules are available for SGL which perform bi-level screening, *i.e.* both group and variable screening [21, 33], but there are no strong rules which perform bi-level screening. The strong screening rule framework proposed by Tibshirani et al. [31] does not fully extend to sparse-group or non-separable penalties, whilst the strong screening rule derived for SGL in Liang et al. [19] applies only group-level screening.

---

### Algorithm 1 Sparse-group screening framework

---

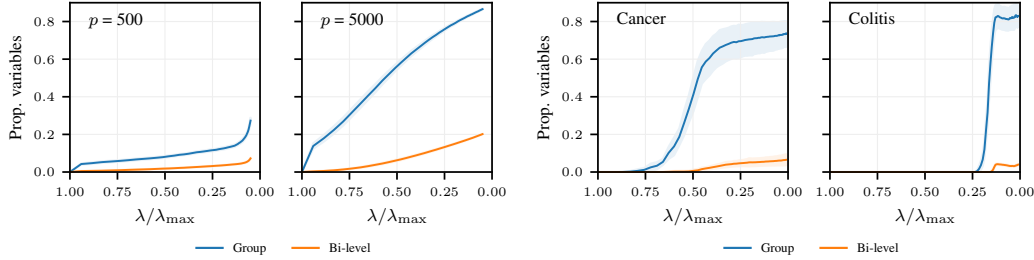
**Input:**  $\lambda \in \mathbb{R}^l$ ,  $\mathbf{X} \in \mathbb{R}^{n \times p}$ ,  $y \in \mathbb{R}^n$   
**for**  $k = 1$  **to**  $l - 1$  **do**  
 $\mathcal{S}_g(\lambda_{k+1}) \leftarrow$  group screening on full input  
 $\mathcal{S}_v(\lambda_{k+1}) \leftarrow$  variable screening on  $g \in \mathcal{S}_g(\lambda_{k+1})$   
 $\mathcal{E}_v \leftarrow \mathcal{S}_v(\lambda_{k+1}) \cup \mathcal{A}_v(\lambda_k)$   
compute  $\hat{\beta}_{\mathcal{E}_v}(\lambda_{k+1})$   
 $\mathcal{K}_v \leftarrow$  variable KKT violations on  $\hat{\beta}(\lambda_{k+1})$   
**while**  $\text{card}(\mathcal{K}_v) > 0$  **do**  
 $\mathcal{E}_v \leftarrow \mathcal{E}_v \cup \mathcal{K}_v$   
compute  $\hat{\beta}_{\mathcal{E}_v}(\lambda_{k+1})$   
 $\mathcal{K}_v \leftarrow$  variable KKT violations on  $\hat{\beta}(\lambda_{k+1})$   
**end while**  
**end for**  
**Output:**  $\hat{\beta}(\lambda_1), \dots, \hat{\beta}(\lambda_l) \in \mathbb{R}^{p \times l}$

---

**Framework.** We introduce a new framework (Algorithm 1) for applying strong screening rules to sparse-group penalties that allow for bi-level screening, based on the framework introduced by Tibshirani et al. [31]. In the sparse-group framework, a screened set of groups is computed,  $\mathcal{S}_g$ , from the full input. An additional layer of screening is then performed to compute  $\mathcal{S}_v$  using  $\mathcal{S}_g$ . This forms the reduced input set for fitting,  $\mathcal{E}_v$ . The aim of finding  $\mathcal{E}_v$  is the same as for the lasso and SLOPE strong rules, but the framework first discards irrelevant groups. KKT checks are performed on  $\mathcal{E}_v$  to ensure no violations have occurred. The framework applied to gSLOPE and SGS is presented in Appendix D.

Based on the framework described in Algorithm 1, the screening rules for SGS are derived (Section 4). The screening rule for gSLOPE (Section 3) follows a similar framework, where  $\mathcal{S}_v$  is taken as all variables within the groups of  $\mathcal{S}_g$ . The KKT checks are then performed only on the groups.

By applying bi-level screening for SGS, a substantially larger proportion of variables are discarded, than if just group screening were applied (Figure 1). Using only group screening for SGS, without the additional variable screening step, resulted in the number of variables in the screened set scaling poorly with increased dimensionality. This demonstrates that bi-level screening effectively manages the scaling of SGS under rising dimensions.



(a) Applied to synthetic data (Section 5.1). Data generated under a linear model for  $p = 500, 5000$ . The results are averaged over 100 repetitions.

(b) Applied to two real genetics datasets (Section 5.2), with groups formed using pathways. The results are averaged over the nine pathway collections.

Figure 1: The proportion of variables in  $\mathcal{S}_v$  relative to the full input for SGS, shown for group and bi-level screening, plotted as a function of the regularization path, with 95% confidence intervals.

### 3 Group SLOPE

The strong screening rule for gSLOPE presented in this section is formulated by computing the zero condition of its subdifferential (as per Equation 3) derived in Theorem 3.1. To derive the subdifferential, we define the operator

$$[b]_{\mathcal{G},q} := (p_1^q \|b^{(1)}\|_2, \dots, p_m^q \|b^{(m)}\|_2)^\top.$$

In particular,  $[b]_{\mathcal{G}_Z, -0.5}$  is the operator applied only to the inactive groups using the quotient  $q = -0.5$ .

**Theorem 3.1** (gSLOPE subdifferential). *The subdifferential for gSLOPE is given by*

$$\partial J_{\text{gslope}}(\beta; w) = \begin{cases} \{x \in \mathbb{R}^{\text{card } \mathcal{G}_Z} : [x]_{\mathcal{G}_Z, -0.5} \in \partial J_{\text{slope}}(0; w_Z)\}, & \text{at } 0. \\ w_g \sqrt{p_g} \frac{\beta^{(g)}}{\|\beta^{(g)}\|_2}, & \text{otherwise.} \end{cases}$$

The choice of  $q = -0.5$  leads to  $J_{\text{gslope}}^*(x; w) = J_{\text{slope}}^*([x]_{\mathcal{G}, -0.5})$ , which allows the gSLOPE subdifferential to be written in terms of the SLOPE one [6]. Combining the KKT conditions (Equation 2) with the gSLOPE subdifferential (Theorem 3.1) reveals that a group is zero if  $h(\lambda) := ([\nabla f(\hat{\beta}(\lambda))]_{\mathcal{G}, -0.5})_\downarrow \in \partial J_{\text{slope}}(\mathbf{0}; \lambda w_Z)$ . Using the subdifferential of SLOPE [17], this is given by

$$\text{cumsum}(h(\lambda) - \lambda w_Z) \preceq \mathbf{0}. \quad (5)$$

This condition is checked efficiently using the algorithm proposed for the SLOPE strong rule (Algorithm A1) leading to the strong rule for gSLOPE (Proposition 3.2). The algorithm assumes that the indices for the inactive predictors will be ordered last in the input  $c$  and the features  $|\hat{\beta}|_\downarrow$  [17].

**Proposition 3.2** (Strong screening rule for gSLOPE). *Taking  $c = h(\lambda_{k+1})$  and  $\phi = \lambda_{k+1} w$  as inputs for Algorithm A1 returns a superset  $\mathcal{S}_g(\lambda_{k+1})$  of the active set  $\mathcal{A}_g(\lambda_{k+1})$ .*

The gradient at path value  $k+1$  is not available for the computation of  $h(\lambda_{k+1})$ , so an approximation is required that does not lead to any violations in Algorithm A1. By the cumsum condition in this algorithm, an approximation for a group  $g$  is sought such that  $h_g(\lambda_{k+1}) \leq h_g(\lambda_k) + R_g$ , where  $R_g \geq 0$  needs to be determined. An approximation is found by assuming that  $h_g(\lambda_{k+1})$  is a Lipschitz function of  $\lambda_{k+1}$  with respect to the  $\ell_1$  norm, that is,

$$|h_g(\lambda_{k+1}) - h_g(\lambda_k)| \leq w_g |\lambda_{k+1} - \lambda_k|.$$

By again noting that  $J_{\text{gslope}}^*(x) = J_{\text{slope}}^*([x]_{\mathcal{G}, -0.5})$ , it can be seen that the assumption is equivalent to those used to derive strong rules for the lasso and SLOPE [17, 31]. By the reverse triangle inequality,

$$|h_g(\lambda_{k+1})| \leq |h_g(\lambda_k)| + \lambda_k w_g - \lambda_{k+1} w_g,$$

leading to the choice  $R_g = \lambda_k w_g - \lambda_{k+1} w_g$  and the gradient approximation strong screening rule.

**Proposition 3.3** (Gradient approximation strong screening rule for gSLOPE). *Taking  $c = h(\lambda_k) + \lambda_k w - \lambda_{k+1} w$  and  $\phi = \lambda_{k+1} w$  as inputs for Algorithm A1, and assuming that for any  $k \in \{1, \dots, l-1\}$ ,*

$$|h_g(\lambda_{k+1}) - h_g(\lambda_k)| \leq w_g |\lambda_{k+1} - \lambda_k|, \quad \forall g = 1, \dots, m,$$

*and  $\mathcal{O}(h(\lambda_{k+1})) = \mathcal{O}(h(\lambda_k))$ , then the algorithm returns a superset  $\mathcal{S}_g(\lambda_{k+1})$  of the active set  $\mathcal{A}_g(\lambda_{k+1})$ .*

## 4 Sparse-group SLOPE

This section presents the group and variable screening rules for SGS. They are derived using the SGS KKT conditions, formulated in terms of SLOPE and gSLOPE (by the sum rule of subdifferentials):

$$-\nabla f(\beta) \in \lambda \alpha \partial J_{\text{slope}}(\beta; v) + \lambda(1 - \alpha) \partial J_{\text{gslope}}(\beta; w). \quad (6)$$

### 4.1 Group screening

For inactive groups, the KKT conditions (Equation 6) for SGS are

$$\begin{aligned} (\nabla f(\beta) + \lambda \alpha \partial J_{\text{slope}}(\mathbf{0}; v))_{\mathcal{G}_Z} &\in \lambda(1 - \alpha) \partial J_{\text{gslope}}(\mathbf{0}; w_Z), \\ \implies \text{cumsum} \left( ([\nabla f(\beta) + \lambda \alpha \partial J_{\text{slope}}(\mathbf{0}; v)]_{\mathcal{G}_Z, -0.5})_{\downarrow} - \lambda(1 - \alpha) w_Z \right) &\preceq \mathbf{0}. \end{aligned} \quad (7)$$

The problem reduces to that of the gSLOPE screening rule (Section 3), with input given by  $c = ([\nabla f(\beta) + \lambda \alpha \partial J_{\text{slope}}(\mathbf{0}; v)]_{\mathcal{G}, -0.5})_{\downarrow}$  and  $\phi = \lambda(1 - \alpha)w$ . To determine the form of the quantity  $\partial J_{\text{slope}}(\mathbf{0}; v)$ , the term inside the  $[\cdot]_{\mathcal{G}_Z, -0.5}$  operator needs to be as small as possible for Equation 7 to be satisfied. This term is found to be the soft thresholding operator,  $S(\nabla f(\beta), \lambda \alpha) := \text{sign}(\nabla f(\beta))(|\nabla f(\beta)| - \lambda \alpha)_+$  (with the derivation presented in Appendix B.2).

By using the soft-thresholding operator, a valuable connection between SGS and SGL is made, as this operator is used in the gradient update step for SGL [29]. Such a connection has the potential to lead to new and more efficient optimization approaches for SGS that are more closely related to those used to solve SGL, similar to the recently developed coordinate descent algorithm for SLOPE [18].

Using this function, the (non-approximated) strong group screening rule for SGS is given in Proposition B.1. Using a similar Lipschitz assumption as for the gSLOPE rule gives the gradient approximation strong group screening rule for SGS (Proposition 4.1).

**Proposition 4.1** (Gradient approximation strong group screening rule for SGS). *Let  $\tilde{h}(\lambda) := ([S(\nabla f(\hat{\beta}(\lambda)), \lambda \alpha)]_{\mathcal{G}, -0.5})_{\downarrow}$ . Taking  $c = \tilde{h}(\lambda_k) + \lambda_k(1 - \alpha)w - \lambda_{k+1}(1 - \alpha)w$  and  $\phi = \lambda_{k+1}(1 - \alpha)w$  as inputs for Algorithm A1, and assuming that for any  $k \in \{1, \dots, l-1\}$ ,*

$$\left| \tilde{h}_g(\lambda_{k+1}) - \tilde{h}_g(\lambda_k) \right| \leq (1 - \alpha) w_g |\lambda_{k+1} - \lambda_k|, \quad \forall g = 1, \dots, m,$$

*and  $\mathcal{O}(\tilde{h}(\lambda_{k+1})) = \mathcal{O}(\tilde{h}(\lambda_k))$ , then the algorithm returns a superset  $\mathcal{S}_g(\lambda_{k+1})$  of  $\mathcal{A}_g(\lambda_{k+1})$ .*

### 4.2 Variable screening

Whilst the group screening for SGS returns a superset,  $\mathcal{S}_g$ , of the active group set, exploiting the sparse-group penalization of SGS allows for the screened set to be further reduced by also applying variable screening. The KKT conditions (Equation 6) for a zero variable,  $j \in \mathcal{G}_g$ , in an active group,  $g \in \mathcal{A}_g$ , are

$$-\nabla_j f(\beta) \in \lambda \alpha \partial J_{\text{slope}}(\mathbf{0}; v_j). \quad (8)$$

The gSLOPE subdifferential term vanishes as the numerator is zero in Theorem 3.1. The problem reduces to that of SLOPE variable screening, applied only to the variables that belong to groups in  $\mathcal{A}_g$  and scaled by  $\alpha$ . The gradient approximated rule is formalized in Proposition 4.2 (the non-approximated version is presented in Proposition B.2).

**Proposition 4.2** (Gradient approximation strong variable screening rule for SGS). *Let  $\bar{h}(\lambda) = (\nabla f(\hat{\beta}(\lambda)))_{|\downarrow|}$ . Taking  $c = |\bar{h}(\lambda_{k+1})| + \lambda_k \alpha v - \lambda_{k+1} \alpha v$  and  $\phi = \lambda_{k+1} \alpha v$  for only the variables in the groups in  $\mathcal{A}_g(\lambda_{k+1})$  as inputs for Algorithm A1, and assuming that for any  $k \in \{1, \dots, l-1\}$ ,*

$$|\bar{h}_j(\lambda_{k+1}) - \bar{h}_j(\lambda_k)| \leq \alpha v_j |\lambda_{k+1} - \lambda_k|, \forall j \in \mathcal{G}_{\mathcal{A}_g(\lambda_{k+1})},$$

*and  $\mathcal{O}(\bar{h}(\lambda_{k+1})) = \mathcal{O}(\bar{h}(\lambda_k))$ , then the algorithm returns a superset  $\mathcal{S}_v(\lambda_{k+1})$  of  $\mathcal{A}_v(\lambda_{k+1})$ .*

In practice  $\mathcal{A}_g(\lambda_{k+1})$  is not available, as this is exactly what we are trying to superset with any screening rule. However, Proposition 4.1 states that it is contained within  $\mathcal{S}_g(\lambda_{k+1})$ , so that the screened set can be used instead and complemented with KKT checks to ensure there are no violations, which would be performed anyway. For the checks, the group KKT conditions (Equation 6) are checked. For any active groups or groups violating the check (indicating that they should be active), the variable KKT conditions (Equation 8) are checked on the variables within those groups, to identify those that need to be added to  $\mathcal{E}_v$ .

## 5 Results

In this section, the effectiveness of the screening rules for gSLOPE and SGS is illustrated through the analysis of both synthetic (Section 5.1) and real data (Section 5.2). Any mentions of  $\mathcal{E}$ ,  $\mathcal{A}$  in reference to group and variable metrics refers to  $\mathcal{E}_g$ ,  $\mathcal{A}_g$  and  $\mathcal{E}_v$ ,  $\mathcal{A}_v$  respectively. For SGS,  $\mathcal{E}_g$  is the groups with representation in  $\mathcal{E}_v$  (the groups fitted). Computational information is presented in Appendix F.1.

### 5.1 Synthetic data analysis

**Set up.** For the synthetic data, a multivariate Gaussian design matrix,  $\mathbf{X} \sim \mathcal{N}(\mathbf{0}, \Sigma) \in \mathbb{R}^{400 \times p}$ , was used and the within-group correlation set to  $\Sigma_{i,j} = \rho$ , where  $i$  and  $j$  belong to the same group. The correlation and number of features were varied between  $\rho \in \{0, 0.3, 0.6, 0.9\}$  and  $p \in \{500, 1625, 2750, 3875, 5000\}$ , producing 20 simulation cases. Each simulation case was repeated 100 times. Two models were considered: linear and logistic. For the linear model, the output was generated as  $y = \mathbf{X}\beta + \mathcal{N}(0, 1)$  and for the logistic model the class probabilities were calculated using  $\sigma(\mathbf{X}\beta + \mathcal{N}(0, 1))$ , where  $\sigma$  is the sigmoid function. Groups of sizes between 3 and 25 were considered, of which 15% were set to active. Within each group, 30% of the variables were set to active with the signal sampled from  $\beta \sim \mathcal{N}(0, 5)$ .

gSLOPE and SGS were each fit along a log-linear path of  $l = 50$  regularization parameters using warm starts. The first path value  $\lambda_1$  was set to the exact value at which the first group enters the model (given in Appendix A.3 for gSLOPE and Appendix B.4 for SGS). The final regularization value was set to  $\lambda_{50} = 0.05\lambda_1$ . The data was  $\ell_2$  standardized and for the linear model an intercept was fitted. Both models had FDR-control parameters set to 0.05, and  $\alpha = 0.95$  for SGS. Even though the models were fit using the adaptive three operator splitting algorithm (ATOS) [26], it should be noted that the screening rules are independent of the choice of fitting algorithm.

Primarily, the results for the linear model are presented, and the corresponding plots for the logistic model are presented in Appendix F.3.2.

**Screening efficiency.** By comparing the sizes of the fitting set ( $\mathcal{E}$ ) to the active set ( $\mathcal{A}$ ), we can understand the difference between the minimum dimensionality needed against the dimensionality provided by the screening rules. As expected, these sizes increase as  $\lambda$  decreases (Figure 2). In particular, the gap between sets widens as more features enter the model. The size of  $\mathcal{E}$  remains far below the size of the full input space even at the lowest value of  $\lambda$ , showing that the screening rules have a benefit along the whole path. This finding is found to be independent of  $\rho$ ,  $p$ , and model fitted (see Appendix F.3). The performance of the screening rules are generally similar across linear and logistic models (Figure 3). As the within-group correlation increases, the size of both the screened and active sets decreases, causing the variables to move in the same direction within the same group. Due to the shape of the convex penalty of SLOPE, highly correlated features are clustered together [36]. This leads to smaller active sets, and in turn, also smaller screened sets. Additionally, it can be seen that the size difference between the screened and active sets decreases with correlation. Across the different correlation values, the linear model had smaller set sizes than the logistic one.

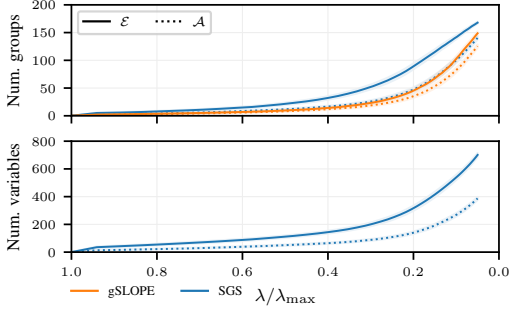


Figure 2: The number of groups/variables in  $\mathcal{E}$ ,  $\mathcal{A}$  for both gSLOPE and SGS as a function of the regularization path for the linear model with  $p = 2750$ ,  $\rho = 0.6$ ,  $m = 197$ . The results are averaged over 100 repetitions, with the shaded regions corresponding to 95% confidence intervals.

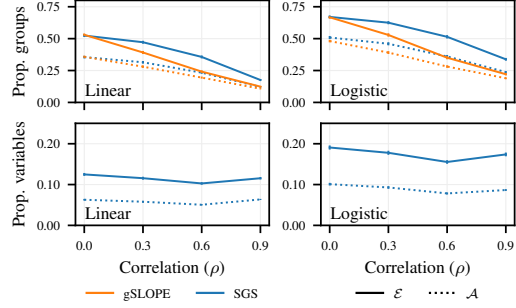


Figure 3: The proportion of groups/variables in  $\mathcal{E}$ ,  $\mathcal{A}$ , relative to the full input, shown for gSLOPE and SGS. This is shown as a function of the correlation ( $\rho$ ), averaged over all cases of the input dimension ( $p$ ), with 100 repetitions for each  $p$ , for both linear and logistic models, with standard errors shown.

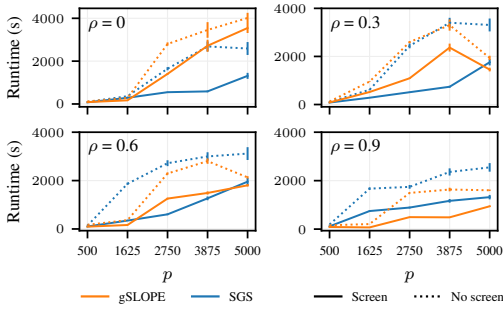


Figure 4: Runtime (in seconds) for fitting 50 models along a path, shown for screening against no screening as a function of  $p$ , broken down into different correlation cases, for the linear model. The results are averaged over 100 repetitions, with standard errors shown.

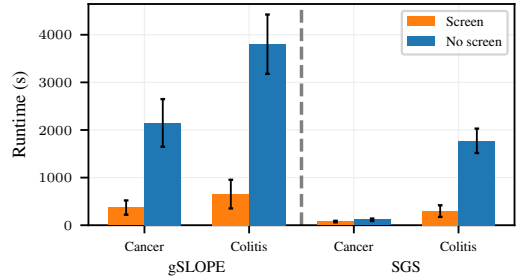


Figure 5: Runtime (in seconds) for fitting 100 models along a path for screening against no screening for gSLOPE and SGS, averaged across the nine collections of pathways for each dataset, with standard errors shown.

**Runtime performance.** A key metric of performance for a screening rule is the time taken to fit a path of models. Increasing the value of  $p$  demonstrates the computational cost reduction of applying a screening rule (Figure 4). For the smaller values of  $p$ , the runtime tends to be similar whether screening is applied or not. However, once the input dimension increases, the benefit of screening can be seen clearly. Additionally, increasing the within-group correlation tends to lead to smaller active and screened sets, but the benefit of screening appears to be robust under different correlations.

A clear improvement with regards to runtime can be seen aggregating the results across all simulation cases (Table 1). In particular, for both models considered, screening halves the runtime for fitting 50 models for SGS.

## 5.2 Real data experiments

**Datasets.** The screening rules were applied to two gene expression datasets with binary responses. The datasets were previously analyzed to measure the predictive performance of sparse-group regression models on large datasets [14, 29]. The *cancer* dataset contains gene data for 60 breast cancer patients who had been treated with tamoxifen for 5 years, classified into binary labels depending on whether the cancer recurred [20]. The *colitis* dataset uses transcriptional profiles in peripheral blood mononuclear cells of 127 patients to determine which patients have an inflammatory bowel disease (ulcerative colitis or Crohn’s). Of the 127 samples, 42 of them are controls [7].

Table 1: Runtime (in seconds) for fitting 50 models along a path, shown for screening against no screening, for the linear and logistic models. The results are averaged across all cases of the correlation ( $\rho$ ) and dimensionality ( $p$ ), with standard errors shown.

Method	Type	Screen (s)	No screen (s)
gSLOPE	Linear	1016 $\pm$ 21	1623 $\pm$ 27
gSLOPE	Logistic	814 $\pm$ 8	1409 $\pm$ 11
SGS	Linear	735 $\pm$ 15	1830 $\pm$ 34
SGS	Logistic	407 $\pm$ 2	859 $\pm$ 6

Table 2: The sizes of the sets  $\mathcal{A}$  and  $\mathcal{E}$  (with standard errors), averaged across 100 path values and pathway collections for each of the two datasets. SGS var/grp shows the corresponding metrics for  $\mathcal{A}_v, \mathcal{E}_v$  and  $\mathcal{A}_g, \mathcal{E}_g$  for the bi-level screening procedure.

Method	Dataset	card( $\mathcal{A}$ )	card( $\mathcal{E}$ )
gSLOPE	Cancer	66 $\pm$ 1	120 $\pm$ 2
gSLOPE	Colitis	32 $\pm$ 1	56 $\pm$ 2
SGS grp	Cancer	50 $\pm$ 1	115 $\pm$ 2
SGS grp	Colitis	18 $\pm$ 1	87 $\pm$ 3
SGS var	Cancer	71 $\pm$ 1	212 $\pm$ 4
SGS var	Colitis	25 $\pm$ 1	209 $\pm$ 6

The genes of both datasets were assigned to pathways (groups) that were obtained from the Molecular Signature Database.<sup>1</sup> Nine collections of pathways were downloaded and as the pathways included different genes, nine unique design matrices for each dataset were created, each with a unique grouping structure. This gave 18 design matrices in total to which the screening rules were applied.

Both gSLOPE and SGS were fitted with their FDR-control parameters set to 0.01 and for SGS  $\alpha = 0.99$ . Each model was fitted along a path of 100 regularization parameters, with  $\lambda_1$  set as described in Appendices A.3 and B.4, and  $\lambda_{100} = 0.01\lambda_1$ . The data was  $\ell_2$  standardized and no intercept was used.

**Results.** For both gSLOPE and SGS, the screening rules lead to considerably faster runtimes (Figure 5). In particular, the use of the screening rules significantly benefits the gSLOPE approach. With the reduced input feature space, any issues with convergence of the fitting algorithm are substantially decreased. For the *cancer* dataset, 186 model fits (out of the 900) did not reach convergence with no screening, compared to only 16 with screening. A similar trend occurred for the *colitis* dataset. As gSLOPE applies no variable penalization, it is forced to fit all variables within a group. For datasets with large groups, such as those considered here, this leads to a problematic fitting process which can include many noisy variables.

The analysis of the real data further illustrates the benefits of the bi-level screening to the runtime and performance of SGS. Figure 1(b) illustrates that for these large genetics datasets, the bi-level screening allows the input dimensionality for SGS to be reduced to a much greater extent than by just group screening.

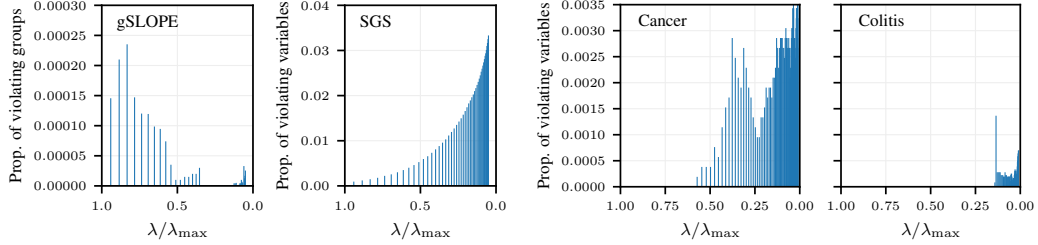
Both screening rules can drastically reduce the input dimensionality as seen in Table 2. For the *colitis* dataset, the SGS screening rule reduces the input dimensionality to just 2% of the full space. This comes without the cost of solution consistency. The estimated model coefficients with and without screening were very close to each other, with their  $\ell_2$  distances of order  $10^{-8}$  (Appendices F.2 and F.4).

### 5.3 KKT violations

The screening rules rely on assumptions that can fail. In these cases, KKT checks are implemented to ensure that no active variables are excluded from  $\mathcal{E}_v$ . A KKT violation occurs when a variable is not included in the screening set,  $\mathcal{S}_v$ , but should be according to the KKT optimality conditions (Equation 2), in which case it is added into the fitting set,  $\mathcal{E}_v$ . KKT violations are very rare for gSLOPE (Figure 6), occurring on the simulated data infrequently toward the start of the path. On the real data, no KKT violations occurred for gSLOPE.

<sup>1</sup><https://www.gsea-msigdb.org/gsea/msigdb/human/collections.jsp>





(a) Group violations for gSLOPE and variable violations for SGS, fitted to linear models, averaged over all cases of  $p$  and the correlation ( $\rho$ ). (b) Variable violations for SGS applied to the *cancer* and *colitis* datasets, averaged over the nine pathway collections.

Figure 6: The proportion of KKT violations relative to the full input space, as a function of the regularization path.

For SGS, KKT violations are more common, as the additional layer of screening carries with it additional assumptions. Additionally, the subdifferential term in Equation 7 was chosen to be as small as possible, leading to tighter screened sets. The increased violations are reflective of this. On both the simulated and real datasets, SGS recorded an increasing number of KKT violations as the fitted models became denser (Figure 6). The shape of the increasing number of KKT violations mirrors the log-linear shape of the regularization path. The trend of increasing KKT violations with denser models is also observed for the SLOPE strong screening rule [17].

Despite the increased number of KKT violations for SGS, which amounts to the additional computational cost of performing the KKT checks and repeated sub-fitting in Algorithm 1, the overall screening procedure still results in substantial runtime improvements, as evidenced in Tables 1 and 2. This shows that screening rules can provide improvements to computational cost, even with assumptions that are often violated.

## 6 Discussion

In this manuscript, we have developed strong screening rules for group-based SLOPE models: Group SLOPE and Sparse-group SLOPE, neither of which have any previous screening rules. The screening rule for gSLOPE screens out irrelevant groups before fitting. The screening rules for SGS perform bi-level screening, based on our proposed sparse-group screening framework.

The two proposed screening rules differ from the existing SLOPE screening rules both in construction and in final outcome. gSLOPE only performs screening through the groups, forcing it to keep all variables within the screened groups, even noisy ones, in the optimization process. SGS, similarly to SLOPE and in contrast to gSLOPE, performs variable screening after its group screening step. As additional assumptions are required for SGS to perform bi-level selection, its computational efficiency is not as effective as the one observed with the SLOPE screening rules [17]. The superiority of SGS in variable selection and predictive performance when group information is available overcomes the additional computational burden [14].

Through comprehensive analysis of synthetic and real data, we illustrate that the screening rules lead to dramatic improvements in the runtime of gSLOPE and SGS models, as well as for group-based OSCAR models (Appendix E). This is achieved without affecting model accuracy. This is particularly important in datasets where  $p \gg n$ , such as genetics ones, which is the main motivation behind SLOPE [4]. The screening rules presented in this manuscript allow group-based SLOPE, and by extension, group-based OWL models, to achieve computational fitting times more in line with lasso-based models, making them more widely accessible.

**Limitations.** One of the limitations of our proposed screening rules for SGS is the number of assumptions made. A future direction includes the exploration of alternative strong screening rules that require fewer assumptions. Alternatively, the development of safe rules, which guarantee that only inactive variables are discarded, could be an avenue for future exploration, potentially incorporating safe and strong rules together in a hybrid rule [32, 37]. A comparison between safe and the proposed strong rules developed in this manuscript could provide further insight into which type of screening is most beneficial for non-separable penalties.

## References

- [1] Talal Ahmed and Waheed U. Bajwa. Exsis: Extended sure independence screening for ultrahigh-dimensional linear models. *Signal Processing*, 159:33–48, 2019. ISSN 0165-1684. doi: <https://doi.org/10.1016/j.sigpro.2019.01.018>.
- [2] Alper Atamturk and Andres Gomez. Safe screening rules for  $\ell_0$ -regression from perspective relaxations. In *Proceedings of the 37th International Conference on Machine Learning*, pages 421–430. PMLR, 2020.
- [3] Runxue Bao, Bin Gu, and Heng Huang. Fast OSCAR and OWL Regression via Safe Screening Rules. In *Proceedings of the 37th International Conference on Machine Learning*, pages 653–663. PMLR, 2020.
- [4] Małgorzata Bogdan, Ewout van den Berg, Chiara Sabatti, Weijie Su, and Emmanuel J Candès. SLOPE—Adaptive variable selection via convex optimization. *The Annals of Applied Statistics*, 9(3), 2015. ISSN 1932-6157. doi: 10.1214/15-AOAS842.
- [5] Howard D. Bondell and Brian J. Reich. Simultaneous Regression Shrinkage, Variable Selection, and Supervised Clustering of Predictors with OSCAR. *Biometrics*, 64(1):115–123, 2008. ISSN 0006-341X. doi: 10.1111/j.1541-0420.2007.00843.x.
- [6] Damian Brzyski, Alexej Gossmann, Weijie Su, and Małgorzata Bogdan. Group SLOPE – Adaptive Selection of Groups of Predictors. *Journal of the American Statistical Association*, 114(525):419–433, 2019. doi: 10.1080/01621459.2017.1411269.
- [7] Michael E Burczynski, Ron L Peterson, Natalie C Twine, Krystyna A Zuberek, Brendan J Brodeur, Lori Casciotti, Vasu Maganti, Padma S Reddy, Andrew Strahs, Fred Immermann, Walter Spinelli, Ulrich Schwertschlag, Anna M Slager, Monette M Cotreau, and Andrew J Dorner. Molecular Classification of Crohn’s Disease and Ulcerative Colitis Patients Using Transcriptional Profiles in Peripheral Blood Mononuclear Cells. *The Journal of Molecular Diagnostics*, 8(1):51–61, 2006. ISSN 15251578. doi: 10.2353/jmoldx.2006.050079.
- [8] Denis Chetverikov, Zhipeng Liao, and Victor Chernozhukov. On cross-validated Lasso in high dimensions. *The Annals of Statistics*, 49(3):1300 – 1317, 2021. doi: 10.1214/20-AOS2000.
- [9] Xavier Dupuis and Patrick J C Tardivel. The Solution Path of SLOPE. Working paper, 2023. URL <https://hal.science/hal-04100441>.
- [10] Bradley Efron, Trevor Hastie, Iain Johnstone, and Robert Tibshirani. Least angle regression. *The Annals of Statistics*, 32(2):407–499, 2004. doi: 10.1214/009053604000000067.
- [11] Laurent El Ghaoui, Vivian Viallon, and Tarek Rabbani. Safe feature elimination in sparse supervised learning. Technical Report UCB/EECS-2010-126, EECS Department, University of California, Berkeley, 2010.
- [12] Clément Elvira and Cédric Herzet. Safe rules for the identification of zeros in the solutions of the SLOPE problem. *SIAM Journal on Mathematics of Data Science*, 5(1):147–173, 2021. doi: 10.1137/21m1457631.
- [13] Jianqing Fan and Jinchi Lv. Sure independence screening for ultrahigh dimensional feature space. *Journal of the Royal Statistical Society: Series B (Statistical Methodology)*, 70(5): 849–911, 2008. doi: <https://doi.org/10.1111/j.1467-9868.2008.00674.x>.
- [14] Fabio Feser and Marina Evangelou. Sparse-group SLOPE: adaptive bi-level selection with FDR-control. *arXiv preprint arXiv:2305.09467*, 2023.
- [15] Darren Homrighausen and Daniel J. McDonald. A study on tuning parameter selection for the high-dimensional lasso. *Journal of Statistical Computation and Simulation*, 88(15):2865–2892, 2018. doi: 10.1080/00949655.2018.1491575.
- [16] H W Kuhn and A W Tucker. Nonlinear programming. In *Proceedings of the Second Berkeley Symposium on Mathematical Statistics and Probability*, pages 481–492, Berkeley, Los Angeles, USA, 1950. University of California Press.

- [17] Johan Larsson, Małgorzata Bogdan, and Jonas Wallin. The strong screening rule for SLOPE. In *Advances in Neural Information Processing Systems*, volume 33, pages 14592–14603. Curran Associates, Inc., 2020.
- [18] Johan Larsson, Quentin Klopfenstein, Mathurin Massias, and Jonas Wallin. Coordinate Descent for SLOPE. *Proceedings of Machine Learning Research*, 206:4802–4821, 2022. ISSN 26403498.
- [19] Xiaoxuan Liang, Aaron Cohen, Anibal Solón Heinsfeld, Franco Pestilli, and Daniel J. McDonald. sparsegl: An R Package for Estimating Sparse Group Lasso. *arXiv preprint arXiv:2208.02942*, 2022.
- [20] Xiao-Jun Ma, Zuncai Wang, Paula D Ryan, Steven J Isakoff, Anne Barmettler, Andrew Fuller, Beth Muir, Gayatry Mohapatra, Ranelle Salunga, J. Todd Tuggle, Yen Tran, Diem Tran, Ana Tassin, Paul Amon, Wilson Wang, Wei Wang, Edward Enright, Kimberly Stecker, Eden Estepa-Sabal, Barbara Smith, Jerry Younger, Ulysses Balis, James Michaelson, Atul Bhan, Karleen Habin, Thomas M Baer, Joan Brugge, Daniel A Haber, Mark G Erlander, and Dennis C Sgroi. A two-gene expression ratio predicts clinical outcome in breast cancer patients treated with tamoxifen. *Cancer Cell*, 5(6):607–616, 2004. ISSN 15356108. doi: 10.1016/j.ccr.2004.05.015.
- [21] Eugene Ndiaye, Olivier Fercoq, Alexandre Gramfort, and Joseph Salmon. GAP Safe Screening Rules for Sparse-Group Lasso. In *Advances in Neural Information Processing Systems*, volume 29. Curran Associates, Inc., 2016.
- [22] Eugene Ndiaye, Olivier Fercoq, Alexandre Gramfort, and Joseph Salmon. Gap Safe screening rules for sparsity enforcing penalties. *Journal of Machine Learning Research*, 18, 2016. ISSN 15337928.
- [23] Renato Negrinho and André F T Martins. Orbit regularization. In *Proceedings of the 27th International Conference on Neural Information Processing Systems*, volume 2, pages 3221–3229. MIT Press, 2014.
- [24] Shunichi Nomura. An Exact Solution Path Algorithm for SLOPE and Quasi-Spherical OSCAR. *arXiv preprint arXiv:2010.15511*, 2020.
- [25] Kohei Ogawa, Yoshiki Suzuki, and Ichiro Takeuchi. Safe screening of non-support vectors in pathwise svm computation. In *Proceedings of the 30th International Conference on Machine Learning*, pages 1382–1390. PMLR, 2013.
- [26] Fabian Pedregosa and Gauthier Gidel. Adaptive three operator splitting. In *Proceedings of the 35th International Conference on Machine Learning*, volume 80 of *Proceedings of Machine Learning Research*, pages 4085–4094. PMLR, 2018.
- [27] Ulrike Schneider and Patrick Tardivel. The Geometry of Uniqueness, Sparsity and Clustering in Penalized Estimation. *Journal of Machine Learning Research*, 23:1–36, 2022.
- [28] Atsushi Shibagaki, Masayuki Karasuyama, Kohei Hatano, and Ichiro Takeuchi. Simultaneous safe screening of features and samples in doubly sparse modeling. In *Proceedings of The 33rd International Conference on Machine Learning*, volume 48 of *Proceedings of Machine Learning Research*, pages 1577–1586. PMLR, 2016.
- [29] Noah Simon, Jerome Friedman, Trevor Hastie, and Robert Tibshirani. A Sparse-Group Lasso. *Journal of Computational and Graphical Statistics*, 22(2):231–245, 2013. ISSN 1061-8600. doi: 10.1080/10618600.2012.681250.
- [30] Robert Tibshirani. Regression Shrinkage and Selection Via the Lasso. *Journal of the Royal Statistical Society: Series B (Methodological)*, 58(1):267–288, 1996. ISSN 00359246. doi: 10.1111/j.2517-6161.1996.tb02080.x.
- [31] Robert Tibshirani, Jacob Bien, Jerome Friedman, Trevor Hastie, Noah Simon, Jonathan Taylor, and Ryan J. Tibshirani. Strong rules for discarding predictors in lasso-type problems. *Journal of the Royal Statistical Society. Series B: Statistical Methodology*, 74(2):245–266, 2010. ISSN 13697412. doi: 10.1111/j.1467-9868.2011.01004.x.

- [32] Chuyi Wang and Patrick Breheny. Adaptive hybrid screening for efficient lasso optimization. *Journal of Statistical Computation and Simulation*, 92(11):2233–2256, 2022. doi: 10.1080/00949655.2021.2025376.
- [33] Jie Wang and Jieping Ye. Two-Layer Feature Reduction for Sparse-Group Lasso via Decomposition of Convex Sets. *Advances in Neural Information Processing Systems*, 3:2132–2140, 2014. ISSN 10495258.
- [34] Jie Wang, Jiayu Zhou, Peter Wonka, and Jieping Ye. Lasso screening rules via dual Polytope Projection. In *Proceedings of the 26th International Conference on Neural Information Processing Systems*, volume 1, pages 1070–1078. Curran Associates Inc., 2013.
- [35] Xiangrong Zeng and Mário A. T. Figueiredo. Decreasing weighted sorted  $\ell_1$  regularization. *IEEE Signal Processing Letters*, 21:1240–1244, 2014.
- [36] Xiangrong Zeng and Mário A T Figueiredo. The atomic norm formulation of OSCAR regularization with application to the Frank-Wolfe algorithm. In *2014 22nd European Signal Processing Conference (EUSIPCO)*, pages 780–784, 2014.
- [37] Yaohui Zeng, Tianbao Yang, and Patrick Breheny. Hybrid safe–strong rules for efficient optimization in lasso-type problems. *Computational Statistics & Data Analysis*, 153:107063, 2021. ISSN 0167-9473. doi: <https://doi.org/10.1016/j.csda.2020.107063>.

# Appendix

## Table of Contents

---

<b>A</b>	<b>Group SLOPE</b>	<b>14</b>
A.1	Penalty weights . . . . .	14
A.2	Theory . . . . .	14
A.3	Path start derivation . . . . .	15
<b>B</b>	<b>Sparse-group SLOPE</b>	<b>17</b>
B.1	Penalty weights . . . . .	17
B.2	Derivation of soft thresholding operator . . . . .	17
B.3	Theory . . . . .	18
B.4	Path start derivation . . . . .	18
<b>C</b>	<b>SLOPE Algorithm</b>	<b>19</b>
<b>D</b>	<b>Screening rule framework</b>	<b>20</b>
D.1	Group SLOPE algorithm . . . . .	20
D.2	SGS algorithm . . . . .	20
<b>E</b>	<b>Group-based OSCAR</b>	<b>21</b>
E.1	Model definition . . . . .	21
E.2	Results . . . . .	21
<b>F</b>	<b>Results</b>	<b>23</b>
F.1	Computational information . . . . .	23
F.2	Model Comparison . . . . .	23
F.3	Additional results from the simulation study . . . . .	23
F.4	Additional results from the real data analysis . . . . .	30

---

## A Group SLOPE

### A.1 Penalty weights

The penalty weights for gSLOPE were derived to provide group FDR-control under orthogonal designs [6]. For the FDR-control parameter  $q_g \in (0, 1)$ , they are given by (where the indexing corresponds to the sorted groups)

$$w_i^{\max} = \max_{j=1, \dots, m} \left\{ \frac{1}{\sqrt{p_j}} F_{\chi_{p_j}}^{-1}(1 - q_g i/m) \right\}, \text{ for } i = 1, \dots, m,$$

where  $F_{\chi_{p_j}}$  is the cumulative distribution function of a  $\chi$  distribution with  $p_j$  degrees of freedom. A relaxation to this sequence is applied in [6], to give

$$w_i^{\text{mean}} = \bar{F}_{\chi_{p_j}}^{-1}(1 - q_g i/m), \text{ where } \bar{F}_{\chi_{p_j}}(x) := \frac{1}{m} \sum_{j=1}^m F_{\chi_{p_j}}(\sqrt{p_j}x). \quad (9)$$

The mean sequence weights defined in Equation 9 are used for all gSLOPE numerical simulations in this manuscript (shown in Figure A1).

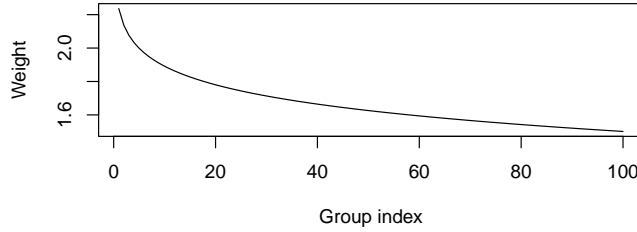


Figure A1: The gSLOPE weights,  $w$ , shown for Figure 4 for  $p = 500, m = 100, q_g = 0.05$ .

### A.2 Theory

*Proof of Theorem 3.1.* The proof is similar to that of Theorem 2.7 in [6], where the subdifferential of gSLOPE is derived under equal groups. It is derived here under more general terms. The subdifferential needs to be derived under two cases:

1. Inactive groups,  $\mathcal{G}_Z$ .
2. Active groups,  $\mathcal{G}_A$ .

*Case 1:* For inactive groups, we consider the subdifferential at zero. The subdifferential of a norm at zero is given by the dual norm of the unit ball [27],

$$\partial J_{\text{gslope}}(\mathbf{0}; w) = \mathbf{B}_{J_{\text{gslope}}^*(\mathbf{0}; w)}[0, 1] = \{x : J_{\text{gslope}}^*(x; w) \leq 1\}.$$

The dual norm for gSLOPE is given by [6]

$$J_{\text{gslope}}^*(x; w) = J_{\text{slope}}^*([x]_{\mathcal{G}, -0.5}).$$

Hence, the dual norm unit ball is

$$\mathbf{B}_{J_{\text{gslope}}^*(\mathbf{0}; w)}[0, 1] = \{x : [x]_{\mathcal{G}, -0.5} \in \mathbf{B}_{J_{\text{slope}}^*(\mathbf{0}; w)}[0, 1]\},$$

where  $\mathbf{B}_{J_{\text{slope}}^*(\mathbf{0}; w)}[0, 1] = \{x \in \mathbb{R}^m : \text{cumsum}(|x|_{\downarrow} - w) \preceq \mathbf{0}\}$  is the unit ball of the dual norm to  $J_{\text{slope}}$  [4]. Using this, the subdifferential at zero for the inactive groups,  $\mathcal{Z}$ , is given by

$$\partial J_{\text{gslope}}(\mathbf{0}; w_Z) = \{x \in \mathbb{R}^{\text{card}(\mathcal{G}_Z)} : [x]_{\mathcal{G}_Z, -0.5} \in \partial J_{\text{slope}}(\mathbf{0}; w_Z)\}.$$

*Case 2:* Without loss of generality, denote the group index  $s$  such that  $\|\beta^{(g)}\|_2 = 0$  for  $g > s$  (inactive groups) and  $\|\beta^{(g)}\|_2 \neq 0$  for  $g \leq s$  (active groups). In other words,  $g \in \mathcal{G}_A$  if  $g \leq s$ . Define a set  $D = \{d \in \mathbb{R}^p : \|\beta^{(1)} + d^{(1)}\|_2 > \dots > \|\beta^{(s)} + d^{(s)}\|_2, \|\beta^{(s)} + d^{(s)}\|_2 > \|d^{(g)}\|_2, g > s\}$ . By definition of a subdifferential, if  $x \in \partial J_{\text{gslope}}(\beta; w)$ , then for all  $d \in D$

$$\sum_{g=1}^m \sqrt{p_g} w_g \|\beta^{(g)} + d^{(g)}\|_2 \geq \sum_{g=1}^m \sqrt{p_g} w_g \|\beta^{(g)}\|_2 + x^\top d.$$

Splitting this up into whether the groups are active (whether  $g \leq s$ ):

$$\begin{aligned} \sum_{g=1}^s \sqrt{p_g} w_g \|\beta^{(g)} + d^{(g)}\|_2 + \sum_{g=s+1}^m \sqrt{p_g} w_g \|d^{(g)}\|_2 &\geq \sum_{g=1}^s \sqrt{p_g} w_g \|\beta^{(g)}\|_2 \\ &+ \sum_{g=1}^s x^{(g)\top} d^{(g)} + \sum_{g=s+1}^m x^{(g)\top} d^{(g)}. \end{aligned} \quad (10)$$

Now, for  $g \in \mathcal{G}_A$ , define a new set  $D_g = \{d \in D : d^{(j)} \equiv \mathbf{0}, j \neq g\}$ . Taking  $d \in D_g$ , Equation 10 becomes

$$\sqrt{p_g} w_g \|\beta^{(g)} + d^{(g)}\|_2 \geq \sqrt{p_g} w_g \|\beta^{(g)}\|_2 + x^{(g)\top} d^{(g)}.$$

Since the set  $\{d^{(g)} : d \in D_g\}$  is open in  $\mathbb{R}^{p_g}$  and contains zero, by Corollary G.1 in [6], it follows that  $x^{(g)} \in \partial f_g(b^{(g)})$  for  $f_g : \mathbb{R}^{p_g} \rightarrow \mathbb{R}, f_g(x) = w_g \sqrt{p_g} \|x\|_2$ . Now, for  $g \leq s$ ,  $f_g$  is differentiable in  $\beta^{(g)}$ , giving

$$x^{(g)} = w_g \sqrt{p_g} \frac{\beta^{(g)}}{\|\beta^{(g)}\|_2},$$

proving the result.  $\square$

*Proof of Proposition 3.2.* Suppose we have  $\mathcal{B} \neq \emptyset$  after running the algorithm. Then, plugging in  $h(\lambda_{k+1}) = ([\nabla f(\hat{\beta}(\lambda_{k+1}))]_{\mathcal{G}, -0.5})_{\downarrow}$  gives

$$\text{cumsum}\left(\left([\nabla f(\hat{\beta}(\lambda_{k+1}))]_{\mathcal{G}, -0.5}\right)_{\downarrow} - \lambda_{k+1} w_{\mathcal{B}}\right) \prec \mathbf{0},$$

so that by the gSLOPE subdifferential (Theorem 3.1) all groups in  $\mathcal{B}$  are inactive. This is valid by the KKT conditions (Equation 2), as we know that  $-\nabla f(\hat{\beta}(\lambda_{k+1})) \in \partial J_{\text{gslope}}(\mathbf{0}; w)$ . Hence,  $\mathcal{S}_g(\lambda_{k+1})$  will contain the active set  $\mathcal{A}_g(\lambda_{k+1})$ .  $\square$

*Proof of Proposition 3.3.* Since  $\text{cumsum}(y) \succeq \text{cumsum}(x) \iff y \succeq x$  [17], we only need to show for a group  $g$ ,

$$|h_g(\lambda_{k+1})| \leq |h_g(\lambda_k)| + \lambda_k w_g - \lambda_{k+1} w_g.$$

Applying the reverse triangle inequality to the Lipschitz assumption gives

$$\begin{aligned} |h_g(\lambda_{k+1})| - |h_g(\lambda_k)| &\leq |h_g(\lambda_{k+1}) - h_g(\lambda_k)| \leq \lambda_k w_g - \lambda_{k+1} w_g \\ \implies |h_g(\lambda_{k+1})| &\leq |h_g(\lambda_k)| + \lambda_k w_g - \lambda_{k+1} w_g, \end{aligned}$$

proving the result.  $\square$

### A.3 Path start derivation

The aim is to find the value of  $\lambda$  at which the first group enters the model. When all features are zero, the gSLOPE KKT conditions (Equation 2) are

$$\mathbf{0} \in \nabla f(\mathbf{0}) + \lambda \partial J_{\text{gslope}}(\mathbf{0}; w).$$

This is satisfied when

$$[\nabla f(\mathbf{0})]_{\mathcal{G}, -0.5} \in \partial J_{\text{slope}}(\mathbf{0}; \lambda w) \implies \text{cumsum}\left(\left([\nabla f(\mathbf{0})]_{\mathcal{G}, -0.5}\right)_{\downarrow} - \lambda w\right) \preceq \mathbf{0}.$$

Rearranging this gives

$$\lambda \succeq \text{cumsum}\left(\left([\nabla f(\mathbf{0})]_{\mathcal{G}, -0.5}\right)_{\downarrow}\right) \oslash \text{cumsum}(w),$$

where  $\oslash$  denotes Hadamard division. Picking the maximum possible  $\lambda$  such that this holds yields

$$\lambda_1 = \max \{ \text{cumsum}([\nabla f(\mathbf{0})]_{\mathcal{G}, -0.5}) \oslash \text{cumsum}(w) \}.$$

This can be verified by noting that  $\lambda_1 = J_{\text{gslope}}^*(\nabla f(\mathbf{0}); w)$  [22]. Now,  $J_{\text{gslope}}^*(x; w) = J_{\text{slope}}^*([x]_{\mathcal{G}, -0.5}; w)$  [6]. The dual norm of SLOPE is given by [23]

$$J_{\text{slope}}^*(x; w) = \max \{ \text{cumsum}(|x|_{\downarrow}) \oslash \text{cumsum}(w) \}.$$

Therefore,  $\lambda_1$  is as before.



## B Sparse-group SLOPE

### B.1 Penalty weights

The penalty weights for SGS provide variable and group FDR-control simultaneously, under orthogonal designs [14]. They are given by (where the indexing corresponds to the sorted variables/groups)

$$v_i^{\max} = \max_{j=1, \dots, m} \left\{ \frac{1}{\alpha} F_{\mathcal{N}}^{-1} \left( 1 - \frac{q_v i}{2p} \right) - \frac{1}{3\alpha} (1 - \alpha) a_j w_j \right\}, \quad i = 1, \dots, p, \quad (11)$$

$$w_i^{\max} = \max_{j=1, \dots, m} \left\{ \frac{F_{\text{FN}}^{-1} \left( 1 - \frac{q_g i}{m} \right) - \alpha \sum_{k \in \mathcal{G}_j} v_k}{(1 - \alpha) p_j} \right\}, \quad i = 1, \dots, m, \quad (12)$$

where  $F_{\chi_{p_j}}$  is the cumulative distribution function of a  $\chi$  distribution with  $p_j$  degrees of freedom,  $F_{\mathcal{N}}$  is the cumulative distribution function of a folded Gaussian distribution, and  $a_j$  is a quantity that requires estimation. The estimator  $\hat{a}_j = \lfloor \alpha p_j \rfloor$  is proposed in [14]. As with gSLOPE (Appendix A.1), a relaxation is possible, giving the weights

$$v_i^{\text{mean}} = \bar{F}_{\mathcal{N}}^{-1} \left( 1 - \frac{q_v i}{2p} \right), \quad \text{where } \bar{F}_{\mathcal{N}}(x) := \frac{1}{m} \sum_{j=1}^m F_{\mathcal{N}} \left( \alpha x + \frac{1}{3} (1 - \alpha) a_j w_j \right), \quad (13)$$

$$w_i^{\text{mean}} = \bar{F}_{\text{FN}}^{-1} \left( 1 - \frac{q_g i}{p} \right), \quad \text{where } \bar{F}_{\text{FN}}(x) := \frac{1}{m} \sum_{j=1}^m F_{\text{FN}} \left( (1 - \alpha) p_j x + \alpha \sum_{k \in \mathcal{G}_j} v_k \right). \quad (14)$$

The mean weights defined in Equations 13 and 14 are used for all SGS numerical simulations in this manuscript (shown in Figure A2).

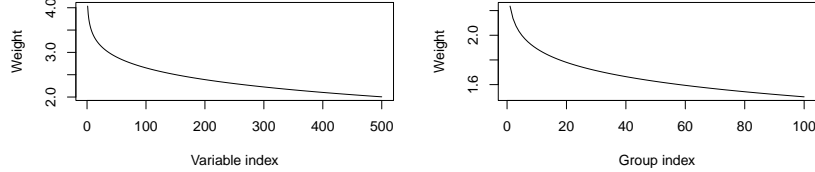


Figure A2: The SGS weights,  $(v, w)$ , shown for Figure 4 for  $p = 500, m = 100, q_v = 0.05, q_g = 0.05, \alpha = 0.95$ .

### B.2 Derivation of soft thresholding operator

To determine the form of the quantity  $\partial J_{\text{slope}}(\mathbf{0}; v)$ , consider that for Equation 7 to be satisfied, the term inside the  $[\cdot]$  operator needs to be as small as possible. Now,

$$\partial J_{\text{slope}}(\mathbf{0}; v) = \{y : \text{cumsum}(|y|) \preceq \text{cumsum}(v)\}.$$

Note that  $\text{cumsum}(y) \preceq \text{cumsum}(x) \iff y \preceq x$ . We consider the cases:

1.  $\nabla_i f(\beta) > \lambda \alpha v_i$ : choose  $y_i = -v_i$ .
2.  $\nabla_i f(\beta) < -\lambda \alpha v_i$ : choose  $y_i = v_i$ .
3.  $\nabla_i f(\beta) \in [-\lambda \alpha v_i, \lambda \alpha v_i]$ : choose  $y_i = \nabla_i f(\beta) / \alpha \lambda$ .

Hence, the term becomes

$$S(\nabla f(\beta), \lambda \alpha) := \text{sign}(\nabla f(\beta)) (|\nabla f(\beta)| - \lambda \alpha)_+,$$

which is the soft thresholding operator.

### B.3 Theory

**Proposition B.1** (Strong group screening rule for SGS). *Let  $\tilde{h}(\lambda) := ([S(\nabla f(\beta), \lambda\alpha)]_{\mathcal{G}, -0.5})_{\downarrow}$ . Then taking  $c = \tilde{h}(\lambda_{k+1})$  and  $\phi = (1 - \alpha)\lambda_{k+1}w$  as inputs for Algorithm A1 returns a superset  $\mathcal{S}_g(\lambda_{k+1})$  of the active set  $\mathcal{A}_g(\lambda_{k+1})$ .*

*Proof of Proposition B.1.* The proof is similar to that of Proposition 3.2. Suppose we have  $\mathcal{B} \neq \emptyset$  after running the algorithm. Then,

$$\begin{aligned} & \text{cumsum}(\tilde{h}_{\mathcal{B}}(\lambda_{k+1}) - \lambda_{k+1}(1 - \alpha)w_{\mathcal{B}}) \prec \mathbf{0} \\ \implies & \text{cumsum}\left(\left([S(\nabla f(\beta), \lambda_{k+1}\alpha)]_{\mathcal{G}, -0.5}\right)_{\downarrow} - \lambda_{k+1}(1 - \alpha)w_{\mathcal{B}}\right) \prec \mathbf{0} \end{aligned}$$

so that by the SGS subdifferential (Equation 7), all groups in  $\mathcal{B}$  are inactive. Hence,  $\mathcal{S}_g(\lambda_{k+1})$  will contain the active set  $\mathcal{A}_g(\lambda_{k+1})$ .  $\square$

*Proof of Proposition 4.1.* The proof is identical to that of Proposition 3.3, replacing  $h_g(\cdot)$  with  $\tilde{h}_g(\cdot)$  and  $\lambda_{k+1}w$  by  $\lambda_{k+1}(1 - \alpha)w$ .  $\square$

**Proposition B.2** (Strong variable screening rule for SGS). *Let  $\bar{h}(\lambda) = |(\nabla f(\hat{\beta}(\lambda)))|_{\downarrow}$ . Then taking  $c = \bar{h}(\lambda_{k+1})$  and  $\phi = \lambda_{k+1}\alpha v$  for only the variables contained in the groups in  $\mathcal{A}_g(\lambda_{k+1})$  in Algorithm A1 returns a superset  $\mathcal{S}_v(\lambda_{k+1})$  of the active set  $\mathcal{A}_v(\lambda_{k+1})$ .*

*Proof.* Suppose we have  $\mathcal{B} \neq \emptyset$  after running the algorithm. Then, we have

$$\text{cumsum}(\bar{h}_{\mathcal{B}}(\lambda_{k+1}) - \lambda_{k+1}\alpha v_{\mathcal{B}}) \prec \mathbf{0} \implies \text{cumsum}\left(\left(|\nabla f(\hat{\beta}(\lambda_{k+1}))|_{\downarrow}\right)_{\mathcal{B}} - \lambda_{k+1}\alpha v_{\mathcal{B}}\right) \prec \mathbf{0}, \quad (15)$$

so that by the SGS subdifferential for non-zero groups (Equation 8), all variables in  $\mathcal{B}$  are inactive. Hence,  $\mathcal{S}_v(\lambda_{k+1})$  will contain the active set  $\mathcal{A}_v(\lambda_{k+1})$ .  $\square$

*Proof for Proposition 4.2.* The proof is identical to that of Proposition 3.3, replacing  $h_g(\cdot)$  with  $\bar{h}_g(\cdot)$ ,  $\lambda_{k+1}v$  with  $\lambda_{k+1}\alpha v$ , and considering only variables in the groups contained in  $\mathcal{A}_g(\lambda_{k+1})$ .  $\square$

### B.4 Path start derivation

The aim is to find the value of  $\lambda$  at which the first variable enters the model. When all features are zero, the SGS KKT conditions (Equation 6) are

$$\begin{aligned} & -\nabla f(\mathbf{0}) \in \lambda(1 - \alpha)\partial J_{\text{gslope}}(\mathbf{0}; w) + \lambda\alpha\partial J_{\text{slope}}(\mathbf{0}; v) \\ \implies & -\frac{1}{\lambda}\nabla f(\mathbf{0}) - (1 - \alpha)\partial J_{\text{gslope}}(\mathbf{0}; w) \in \alpha\partial J_{\text{slope}}(\mathbf{0}; v) \\ \implies & \text{cumsum}\left(\left|-\frac{1}{\lambda}\nabla f(\mathbf{0}) - (1 - \alpha)\partial J_{\text{gslope}}(\mathbf{0}; w)\right|_{\downarrow} - \alpha v\right) \preceq \mathbf{0}. \end{aligned}$$

By the reverse triangle inequality and ordering of the group weights

$$\begin{aligned} & \frac{1}{\lambda}\text{cumsum}(|\nabla f(\mathbf{0})|_{\downarrow}) \preceq \text{cumsum}((1 - \alpha)|\partial J_{\text{gslope}}(\mathbf{0}; w)| - \alpha v) \\ \implies & \lambda \succeq \text{cumsum}(|\nabla f(\mathbf{0})|_{\downarrow}) \oslash \text{cumsum}((1 - \alpha)|\partial J_{\text{gslope}}(\mathbf{0}; w)| - \alpha v). \end{aligned}$$

Now, note that for  $x \in J_{\text{gslope}}(\mathbf{0}; w)$ , it holds

$$\text{cumsum}([x]_{\mathcal{G}, -0.5} - w) \preceq \mathbf{0} \implies [x]_{\mathcal{G}, -0.5} \preceq w \implies \|x^{(g)}\|_2 \leq \sqrt{p_g}w_g, \forall g \in \mathcal{G}.$$

This is satisfied at the upper limit at  $x = \tau\omega$ , where  $\tau$  and  $\omega$  are expanded vectors of the group sizes ( $\sqrt{p_g}$ ) and penalty weights ( $w_g$ ) to  $p$  dimensions, so that each variable within the same group is assigned the same value. Hence,

$$\lambda_1 = \max\{\text{cumsum}(|\nabla f(\mathbf{0})|_{\downarrow}) \oslash \text{cumsum}((1 - \alpha)\tau\omega - \alpha v)\}.$$

## C SLOPE Algorithm

---

**Algorithm A1** Cumsum algorithm from [17]

---

**Input:**  $c \in \mathbb{R}^p, \phi \in \mathbb{R}^p$ , where  $\phi_1 \geq \dots \geq \phi_p \geq 0$   
 $\mathcal{S}, \mathcal{B} \leftarrow \emptyset$   
**for**  $i = 1$  **to**  $p$  **do**  
     $\mathcal{B} \leftarrow \mathcal{B} \cup \{i\}$   
    **if**  $\text{cumsum}(c_{\mathcal{B}} - \phi_{\mathcal{B}}) \geq 0$  **then**  
         $\mathcal{S} \leftarrow \mathcal{S} \cup \mathcal{B}$   
         $\mathcal{B} \leftarrow \emptyset$   
    **end if**  
**end for**  
**Output:**  $\mathcal{S}$

---

## D Screening rule framework

### D.1 Group SLOPE algorithm

For the following is performed for  $k = 1, \dots, l - 1$ :

1. Set  $\mathcal{E}_g = \mathcal{S}_g(\lambda_{k+1}) \cup \mathcal{A}_g(\lambda_k)$ , where  $\mathcal{S}_g(\lambda_{k+1})$  is obtained using Proposition 3.3.
2. Compute  $\hat{\beta}(\lambda_{k+1})$  by Equation 1 with the gSLOPE norm using only the groups in  $\mathcal{E}_g$ . For any groups not in  $\mathcal{E}_g$ ,  $\hat{\beta}(\lambda_{k+1})$  is set to zero.
3. Check the KKT conditions (Equation 2) for all groups at this solution.
4. If there are no violations, we are done and keep  $\hat{\beta}(\lambda_{k+1})$ . Otherwise, add the violating groups into  $\mathcal{E}$  and return to Step 2.

### D.2 SGS algorithm

For the following is performed for  $k = 1, \dots, l - 1$ :

1. *Group screen step*: Calculate  $\mathcal{S}_g(\lambda_{k+1})$  using Proposition 4.1.
2. *Variable screen step*: Set  $\mathcal{E}_v = \mathcal{S}_v(\lambda_{k+1}) \cup \mathcal{A}_v(\lambda_k)$ , where  $\mathcal{S}_v(\lambda_{k+1})$  is obtained using Proposition 4.2 with only the groups in  $\mathcal{S}_g(\lambda_{k+1})$ .
3. Compute  $\hat{\beta}(\lambda_{k+1})$  by Equation 1 with the SGS norm using only the features in  $\mathcal{E}_v$ . For features not in  $\mathcal{E}_v$ ,  $\hat{\beta}(\lambda_{k+1})$  is set to zero.
4. Check the KKT conditions (Equation 6) for all features at this solution.
5. If there are no violations, we are done and keep  $\hat{\beta}(\lambda_{k+1})$ , otherwise add in the violating variables into  $\mathcal{E}_g$  and return to Step 3.

## E Group-based OSCAR

This section presents an extension of the proposed screening rules for group-based OSCAR models. Firstly the OSCAR models are presented, and subsequently, the performance of the screening rules on synthetic data is presented.

### E.1 Model definition

The Ordered Weighted  $\ell_1$  (OWL) framework is defined as [35]

$$\hat{\beta} = \arg \min_{\beta} \{ \nabla f(\beta) + \lambda J_{\text{owl}}(\beta; v) \},$$

where  $J_{\text{owl}}(\beta; v) = \sum_{i=1}^p v_i |\beta|_{(i)}$ ,  $|\beta|_{(1)} \geq \dots \geq |\beta|_{(p)}$ , and  $v$  are non-negative non-increasing weights. SLOPE is a special case of OWL where the weights are taken to be the Benjamini-Hochberg critical values [4]. Octagonal Shrinkage and Clustering Algorithm for Regression (OSCAR) [5] is a further special case of OWL (often referred to as OWL with linear decay) where for a variable  $i$ , the weights are taken to be  $v_i = \sigma_1 + \sigma_2(p - i)$ , and  $\sigma_1, \sigma_2$  are to be set. In Bao et al. [3] they are set to  $\sigma_1 = d_i \|\mathbf{X}^\top y\|_\infty$ ,  $\sigma_2 = \sigma_1/p$ , where  $d_i = i \times e^{-2}$ .

Group OSCAR (gOSCAR) and Sparse-group OSCAR (SGO) are defined using the frameworks provided by gSLOPE [6] and SGS [14], respectively, but instead using the weights (for a variable  $i$  and a group  $g$ )

$$v_i = \sigma_1 + \sigma_2(p - i), \quad w_g = \sigma_1 + \sigma_3(m - g), \quad \sigma_3 = \sigma_1/m. \quad (16)$$

with the weights visualised in Figure A3.

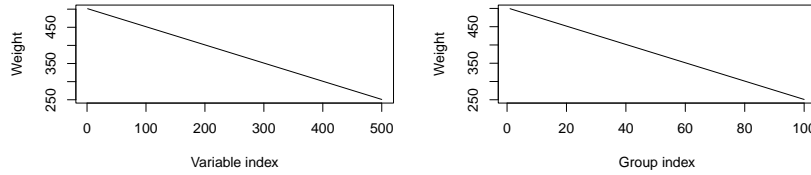


Figure A3: The SGO weights,  $(v, w)$ , shown for Figure 4 for  $p = 500$ ,  $m = 100$ ,  $q_v = 0.05$ ,  $q_g = 0.05$ ,  $\alpha = 0.95$ .

### E.2 Results

Similar observations and conclusions made for the screening rules of gSLOPE and SGS are made for gOSCAR and SGO (Figures A4 - A8).

Figure A4 illustrates the effectiveness of the bi-level screening of SGO, similar to the effectiveness observed for SGS. Figures A5 - A6 showcase the efficiency of the screening rules on the proportion of the selected groups/variables. The screening rules are found to be effective across different data characteristics, with the running time of the models significantly decreasing (Figure A7). Similarly to SGS, KKT violations are more common compared to the ones observed for gOSCAR (Figure A8). This is due to the additional assumptions made at the additional screening layer of SGO and SGS. Similarly to Figure 6(a), the shape of the increasing number of KKT violations mirrors the log-linear shape of the regularization path.

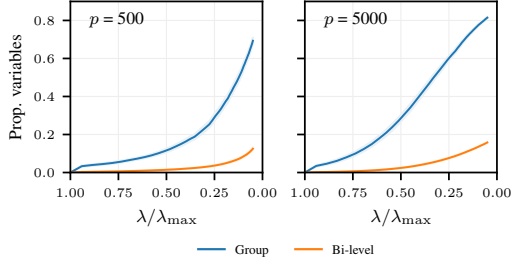


Figure A4: The proportion of variables in  $\mathcal{S}_v$  relative to the full input for SGO, shown for group and bi-level screening plotted as a function of the regularization path, applied to the synthetic data (Section 5.1). The data are generated under a linear model for  $p = 500, 5000$ . The results are averaged over 100 repetitions and 95% confidence intervals are shown (the SGO equivalent of Figure 1 (a)).

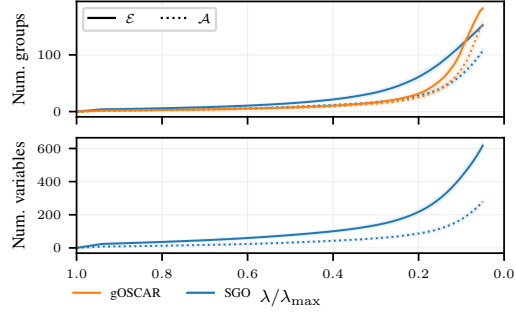


Figure A5: The number of groups/variables in  $\mathcal{E}, \mathcal{A}$  for both gOSCAR and SGO as a function of the regularization path for the linear model with  $p = 2750, \rho = 0.6, m = 197$ . The results are averaged over 100 repetitions, with the shaded regions corresponding to 95% confidence intervals (the gOSCAR/SGO equivalent of Figure 2).

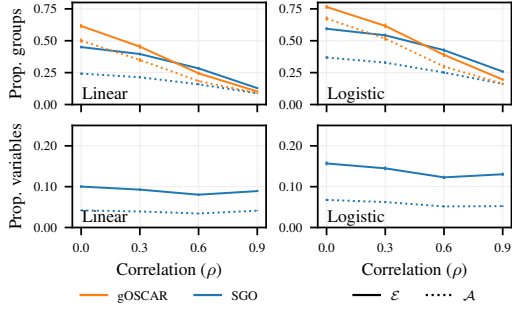


Figure A6: The proportion of groups/variables in  $\mathcal{E}, \mathcal{A}$ , relative to the full input, shown for gOSCAR and SGO. This is shown as a function of the correlation ( $\rho$ ), averaged over all cases of the input dimension ( $p$ ), with 100 repetitions for each  $p$ , for both linear and logistic models, with standard errors shown (the gOSCAR/SGO equivalent of Figure 3).

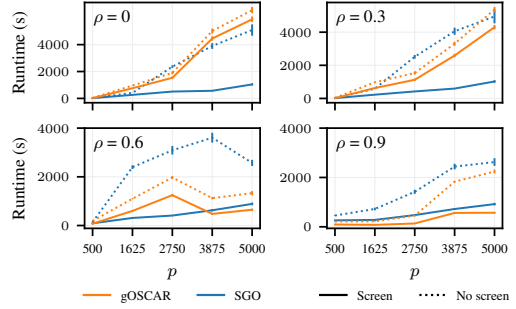


Figure A7: Runtime (in seconds) for fitting 50 models along a path, shown for screening against no screening as a function of  $p$ , broken down into different correlation cases, for the linear model. The results are averaged over 100 repetitions, with standard errors shown (the OSCAR equivalent of Figure 4).

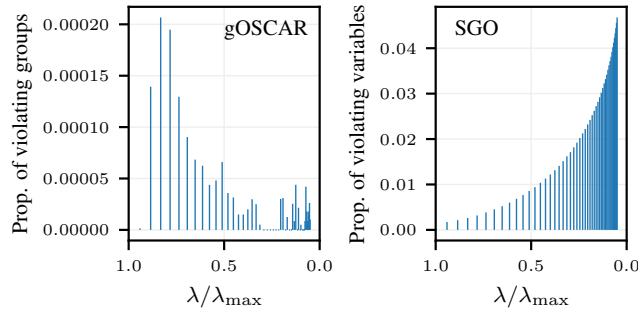


Figure A8: The proportion of KKT violations relative to the full input space, as a function of the regularization path. Group violations for gOSCAR and variable violations for SGS, fitted to linear models, averaged over all cases of  $p$  and  $\rho$  (the gOSCAR/SGO equivalent of Figure 6(a)).

## F Results

### F.1 Computational information

The simulated experiments were executed on a high-performance computing cluster (x86-64 Linux GNU) and the real data analysis was conducted on a Apple Macbook Air (M1, 8GB).

### F.2 Model Comparison

This section presents the accuracy of the models with and without screening, by comparing the  $\ell_2$  distances observed between the screened and non-screened fitted values.

**Synthetic data.** For the linear model, the maximum  $\ell_2$  distances observed between the screened and non-screened fitted values were of order  $10^{-5}$  for gSLOPE and  $10^{-8}$  for SGS (Table A2). Across the different cases, 98000 models were fit in total for each approach (excluding the models for  $\lambda_1$ , where no screening is applied). Of these model fits, there were no instances for gSLOPE where  $\mathcal{E}$  was not a superset of  $\mathcal{A}$ . There was only one instance (out of the 98000) that this occurred for SGS, where  $\mathcal{E}$  was missing a single variable contained in  $\mathcal{A}$  (which had a non-screen fitted value of  $\hat{\beta} = -0.004$ ).

For the logistic model, the maximum  $\ell_2$  distances observed between the screened and non-screened fitted values were of order  $10^{-8}$  for both gSLOPE and SGS (Table A6). Across the different cases, 98000 models were fit in total for each approach (excluding the models for  $\lambda_1$ , where no screening is applied). Of these model fits, there were no instances for gSLOPE or SGS where  $\mathcal{E}$  was not a superset of  $\mathcal{A}$ .

**Real data.** In the real data analysis, the estimated coefficients with and without screening were very close to each other (with  $\ell_2$  to be of order  $10^{-8}$ ) for both SGS and gSLOPE (Table A8). No instances occurred where  $\mathcal{E}$  was not a superset of  $\mathcal{A}$ .

### F.3 Additional results from the simulation study

Table A1: Variable screening metrics for SGS using linear and logistic models for the simulation study presented in Section 5.1. The number of variables in  $\mathcal{A}_v$ ,  $\mathcal{S}_v$ ,  $\mathcal{E}_v$ , and  $\mathcal{K}_v$  are shown, averaged across all 20 cases of the correlation ( $\rho$ ) and  $p$ . Standard errors are shown.

METHOD	TYPE	card( $\mathcal{A}_v$ )	card( $\mathcal{S}_v$ )	card( $\mathcal{E}_v$ )	card( $\mathcal{K}_v$ )
SGS	LINEAR	179 $\pm$ 3	313 $\pm$ 5	363 $\pm$ 6	51 $\pm$ 1
SGS	LOGISTIC	230 $\pm$ 3	405 $\pm$ 5	472 $\pm$ 6	66 $\pm$ 1

Table A2: General and group screening metrics for SGS and gSLOPE using linear and logistic models for the simulation study presented in Section 5.1. General metrics: the runtime (in seconds) for screening against no screening, the number of fitting iterations for screening against no screening, and the  $\ell_2$  distance between the fitted values obtained with screening and no screening. Group screening metrics: the number of groups in  $\mathcal{A}_g$ ,  $\mathcal{S}_g$ ,  $\mathcal{E}_g$ , and  $\mathcal{K}_g$ . The results are averaged across all 20 cases of the correlation ( $\rho$ ) and  $p$ . Standard errors are shown.

METHOD	TYPE	RUNTIME	RUNTIME	card( $\mathcal{A}_g$ )	card( $\mathcal{S}_g$ )	card( $\mathcal{E}_g$ )	card( $\mathcal{K}_g$ )	NUM IT	NUM IT	$\ell_2$ DIST
		(S)	(S)					NO	SCREEN	TO NO
GSLOPE	LINEAR	1016 $\pm$ 21	1623 $\pm$ 27	55 $\pm$ 1	76 $\pm$ 1	76 $\pm$ 1	0.006 $\pm$ 0.004	333 $\pm$ 6	351 $\pm$ 6	2 $\times$ 10 <sup>-6</sup> $\pm$ 1 $\times$ 10 <sup>-6</sup>
GSLOPE	LOGISTIC	814 $\pm$ 8	1409 $\pm$ 11	71 $\pm$ 1	97 $\pm$ 1	97 $\pm$ 1	0.014 $\pm$ 0.014	78 $\pm$ 1	83 $\pm$ 1	1 $\times$ 10 <sup>-8</sup> $\pm$ 1 $\times$ 10 <sup>-8</sup>
SGS	LINEAR	735 $\pm$ 15	1830 $\pm$ 34	61 $\pm$ 1	84 $\pm$ 1	91 $\pm$ 1	21 $\pm$ 1	91 $\pm$ 3	708 $\pm$ 12	2 $\times$ 10 <sup>-9</sup> $\pm$ 3 $\times$ 10 <sup>-9</sup>
SGS	LOGISTIC	407 $\pm$ 2	859 $\pm$ 6	84 $\pm$ 1	107 $\pm$ 1	118 $\pm$ 1	22 $\pm$ 0.3	7 $\pm$ 0.2	51 $\pm$ 0.8	4 $\times$ 10 <sup>-9</sup> $\pm$ 3 $\times$ 10 <sup>-10</sup>



### F.3.1 Additional results for the linear model

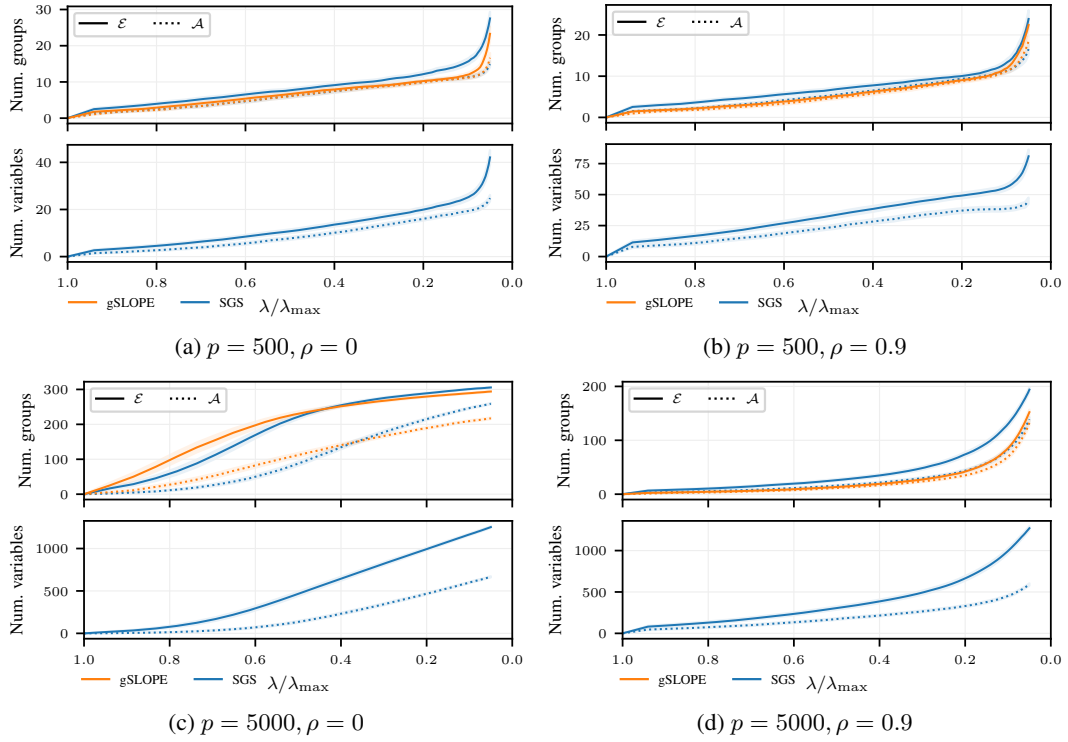


Figure A9: The number of groups/variables in  $\mathcal{E}, \mathcal{A}$  as a function of the regularization path for the linear model with SGS and gSLOPE, shown for different values of the correlation ( $\rho$ ) and  $p$ . The results are averaged over 100 repetitions, with 95% confidence intervals shown.

Table A3: Variable screening metrics for SGS using a linear model for the simulation study presented in Section 5.1. The number of variables in  $\mathcal{A}_v$ ,  $\mathcal{S}_v$ ,  $\mathcal{E}_v$ , and  $\mathcal{K}_v$  are shown. The results are shown for different values of  $p$ , averaged across  $\rho \in \{0, 0.3, 0.6, 0.9\}$ . Standard errors are shown.

METHOD	$p$	$\text{card}(\mathcal{A}_v)$	$\text{card}(\mathcal{S}_v)$	$\text{card}(\mathcal{E}_v)$	$\text{card}(\mathcal{K}_v)$
SGS	500	$19 \pm 1$	$24 \pm 1$	$28 \pm 1$	$4 \pm 0.2$
SGS	1625	$83 \pm 3$	$138 \pm 5$	$161 \pm 6$	$22 \pm 1$
SGS	2750	$188 \pm 7$	$316 \pm 10$	$370 \pm 12$	$54 \pm 2$
SGS	3875	$268 \pm 9$	$470 \pm 14$	$548 \pm 16$	$78 \pm 3$
SGS	5000	$334 \pm 10$	$618 \pm 17$	$712 \pm 20$	$95 \pm 3$

Table A4: General and group screening metrics for SGS and gSLOPE using linear models for the simulation study presented in Section 5.1. General metrics: the runtime (in seconds) for screening against no screening, the number of fitting iterations for screening against no screening, and the  $\ell_2$  distance between the fitted values obtained with screening and no screening. Group screening metrics: the number of groups in  $\mathcal{A}_g$ ,  $\mathcal{S}_g$ ,  $\mathcal{E}_g$ , and  $\mathcal{K}_g$ . The results are shown for different values of  $p$ , averaged across  $\rho \in \{0, 0.3, 0.6, 0.9\}$ . Standard errors are shown.

METHOD	$p$	RUNTIME (S)		$\text{card}(\mathcal{A}_g)$	$\text{card}(\mathcal{S}_g)$	$\text{card}(\mathcal{E}_g)$	$\text{card}(\mathcal{K}_g)$	NUM IT		$\ell_2$ DIST	
		SCREEN	NO SCREEN					SCREEN	NO SCREEN	TO SCREEN	NO SCREEN
gSLOPE	500	$89 \pm 1$	$144 \pm 1$	$9 \pm 0.2$	$10 \pm 0.3$	$10 \pm 0.3$	$0.005 \pm 0.005$	$47 \pm 1$	$55 \pm 1$	$6 \times 10^{-6}$	$7 \times 10^{-6}$
gSLOPE	1625	$231 \pm 5$	$453 \pm 5$	$26 \pm 1$	$36 \pm 1$	$36 \pm 1$	$0.005 \pm 0.006$	$203 \pm 6$	$222 \pm 6$	$1 \times 10^{-6}$	$1 \times 10^{-6}$
gSLOPE	2750	$1061 \pm 15$	$2296 \pm 25$	$56 \pm 2$	$75 \pm 2$	$75 \pm 2$	$0.004 \pm 0.005$	$270 \pm 9$	$350 \pm 9$	$5 \times 10^{-7}$	$7 \times 10^{-7}$
gSLOPE	3875	$1765 \pm 83$	$2800 \pm 113$	$82 \pm 3$	$114 \pm 3$	$114 \pm 3$	$0.006 \pm 0.008$	$549 \pm 19$	$546 \pm 18$	$3 \times 10^{-7}$	$5 \times 10^{-7}$
gSLOPE	5000	$1937 \pm 63$	$2422 \pm 66$	$102 \pm 3$	$147 \pm 4$	$147 \pm 4$	$0.007 \pm 0.012$	$594 \pm 21$	$581 \pm 19$	$2 \times 10^{-7}$	$3 \times 10^{-7}$
SGS	500	$94 \pm 1$	$133 \pm 2$	$9 \pm 0.2$	$11 \pm 0.3$	$12 \pm 0.3$	$3 \pm 0.2$	$28 \pm 1$	$74 \pm 3$	$5 \times 10^{-10}$	$4 \times 10^{-10}$
SGS	1625	$416 \pm 8$	$1129 \pm 19$	$25 \pm 1$	$37 \pm 1$	$41 \pm 1$	$12 \pm 0.3$	$62 \pm 7$	$511 \pm 21$	$2 \times 10^{-9}$	$2 \times 10^{-9}$
SGS	2750	$639 \pm 14$	$2137 \pm 47$	$62 \pm 2$	$82 \pm 2$	$89 \pm 3$	$20 \pm 1$	$80 \pm 6$	$791 \pm 28$	$2 \times 10^{-9}$	$6 \times 10^{-9}$
SGS	3875	$939 \pm 31$	$2862 \pm 96$	$93 \pm 3$	$124 \pm 3$	$136 \pm 4$	$30 \pm 1$	$112 \pm 8$	$1049 \pm 34$	$5 \times 10^{-9}$	$1 \times 10^{-8}$
SGS	5000	$1586 \pm 66$	$2891 \pm 128$	$119 \pm 4$	$164 \pm 3$	$180 \pm 4$	$39 \pm 1$	$171 \pm 11$	$1118 \pm 37$	$2 \times 10^{-9}$	$4 \times 10^{-9}$

### F.3.2 Additional results for the logistic model

This section presents additional results for the logistic model. Similar trends to the ones observed for the linear model are seen.

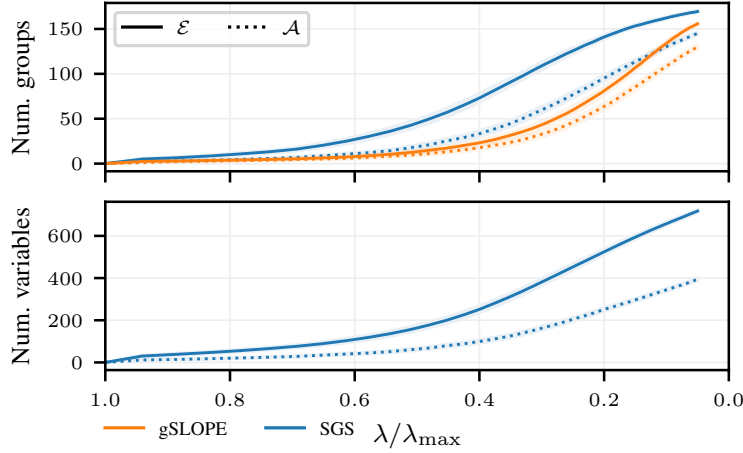


Figure A10: The number of groups/variables in  $\mathcal{E}$ ,  $\mathcal{A}$  as a function of the regularization path for the logistic model with  $p = 2750, \rho = 0.6, m = 197$ , shown for gSLOPE and SGS. The results are averaged over 100 repetitions, with 95% confidence intervals shown. This figure is the equivalent of Figure 2 for the logistic model.

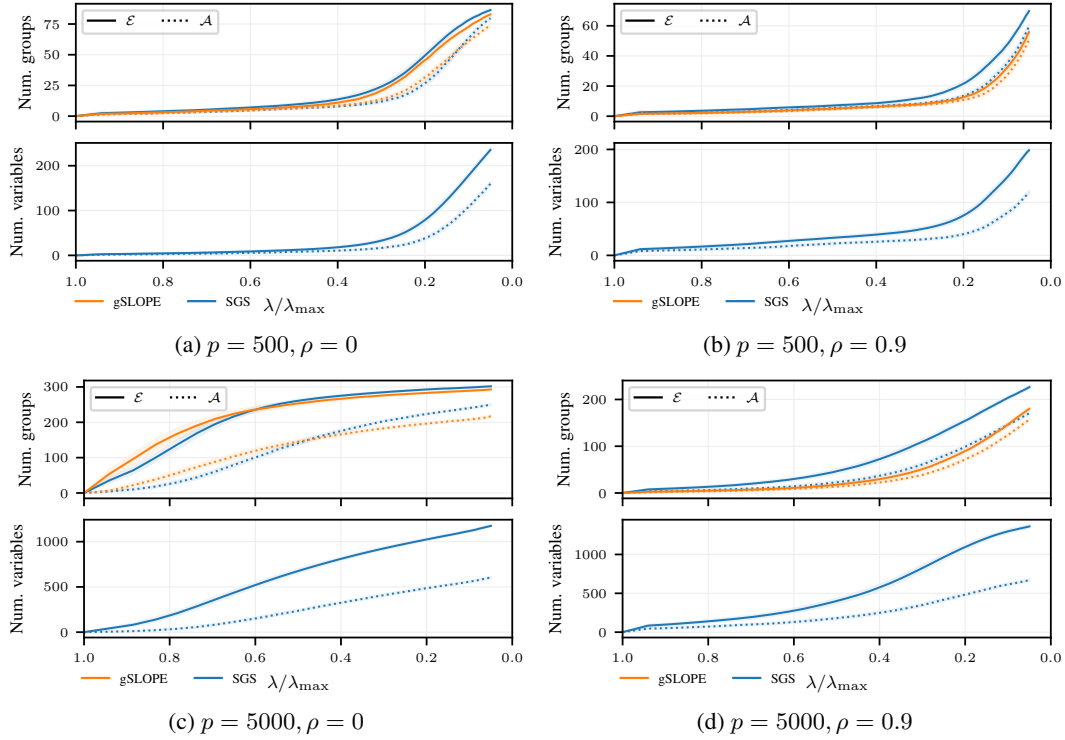


Figure A11: The number of groups/variables in  $\mathcal{E}$ ,  $\mathcal{A}$  as a function of the regularization path for the logistic model with SGS and gSLOPE, shown for different values of the correlation ( $\rho$ ) and  $p$ . The results are averaged over 100 repetitions, with 95% confidence intervals shown.

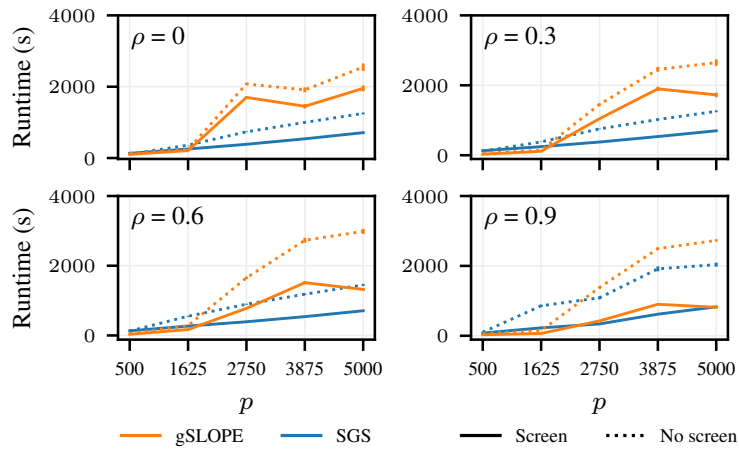


Figure A12: Runtime (in seconds) for screening against no screening as a function of  $p$ , broken down into different correlation cases, for the logistic model. The results are averaged over 100 repetitions, with standard errors shown.

Table A5: Variable screening metrics for SGS using a logistic model for the simulation study presented in Section 5.1. The number of variables in  $\mathcal{A}_v$ ,  $\mathcal{S}_v$ ,  $\mathcal{E}_v$ , and  $\mathcal{K}_v$  are shown. The results are shown for different values of  $p$ , averaged across  $\rho \in \{0, 0.3, 0.6, 0.9\}$ . Standard errors are shown.

METHOD	$p$	$\text{card}(\mathcal{A}_v)$	$\text{card}(\mathcal{S}_v)$	$\text{card}(\mathcal{E}_v)$	$\text{card}(\mathcal{K}_v)$
SGS	500	53 ± 2	71 ± 3	89 ± 4	19 ± 1
SGS	1625	157 ± 5	248 ± 8	291 ± 9	44 ± 1
SGS	2750	247 ± 7	420 ± 11	491 ± 13	71 ± 2
SGS	3875	316 ± 9	571 ± 14	663 ± 16	92 ± 3
SGS	5000	375 ± 10	717 ± 16	824 ± 19	107 ± 3

Table A6: General and group screening metrics for SGS and gSLOPE using logistic models for the simulation study presented in Section 5.1. General metrics: the runtime (in seconds) for screening against no screening, the number of fitting iterations for screening against no screening, and the  $\ell_2$  distance between the fitted values obtained with screening and no screening. Group screening metrics: the number of groups in  $\mathcal{A}_g$ ,  $\mathcal{S}_g$ ,  $\mathcal{E}_g$ , and  $\mathcal{K}_g$ . The results are shown for different values of  $p$ , averaged across  $\rho \in \{0, 0.3, 0.6, 0.9\}$ . Standard errors are shown.

METHOD	$p$	RUNTIME (S)		card( $\mathcal{A}_g$ )		card( $\mathcal{S}_g$ )		card( $\mathcal{E}_g$ )		card( $\mathcal{K}_g$ )		NUM IT		$\ell_2$ DIST	
		SCREEN	NO SCREEN	SCREEN	NO SCREEN	SCREEN	NO SCREEN	SCREEN	NO SCREEN	SCREEN	NO SCREEN	SCREEN	NO SCREEN	TO SCREEN	NO SCREEN
GSLOPE	500	49 ± 1	76 ± 1	26 ± 1	31 ± 1	31 ± 1	31 ± 1	31 ± 1	31 ± 1	0.003 ± 0.004	31 ± 1	40 ± 1	4 × 10 <sup>-8</sup>	5 × 10 <sup>-8</sup>	
GSLOPE	1625	138 ± 3	203 ± 3	43 ± 1	54 ± 2	54 ± 2	54 ± 2	54 ± 2	54 ± 2	0.004 ± 0.006	78 ± 2	79 ± 1	1 × 10 <sup>-8</sup>	5 × 10 <sup>-9</sup>	
GSLOPE	2750	987 ± 11	1641 ± 16	72 ± 2	95 ± 3	95 ± 3	95 ± 3	95 ± 3	95 ± 3	0.008 ± 0.013	87 ± 2	89 ± 1	1 × 10 <sup>-8</sup>	5 × 10 <sup>-9</sup>	
GSLOPE	3875	1441 ± 26	2398 ± 31	98 ± 3	135 ± 3	135 ± 3	135 ± 3	135 ± 3	135 ± 3	0.031 ± 0.054	95 ± 2	98 ± 1	7 × 10 <sup>-9</sup>	3 × 10 <sup>-9</sup>	
GSLOPE	5000	1454 ± 29	2727 ± 40	118 ± 3	168 ± 4	168 ± 4	168 ± 4	168 ± 4	168 ± 4	0.022 ± 0.041	101 ± 2	109 ± 1	4 × 10 <sup>-9</sup>	1 × 10 <sup>-9</sup>	
SGS	500	118 ± 1	113 ± 1	28 ± 1	33 ± 1	33 ± 1	33 ± 1	38 ± 1	38 ± 1	8 ± 0.2	6 ± 0.3	29 ± 1	8 × 10 <sup>-9</sup>	7 × 10 <sup>-10</sup>	
SGS	1625	248 ± 2	538 ± 9	50 ± 2	59 ± 2	59 ± 2	59 ± 2	64 ± 2	64 ± 2	11 ± 0.4	7 ± 1	63 ± 3	5 × 10 <sup>-9</sup>	1 × 10 <sup>-9</sup>	
SGS	2750	374 ± 2	868 ± 12	85 ± 3	104 ± 2	104 ± 2	104 ± 2	115 ± 3	115 ± 3	21 ± 1	7 ± 0.4	57 ± 2	3 × 10 <sup>-9</sup>	5 × 10 <sup>-10</sup>	
SGS	3875	558 ± 4	1280 ± 19	116 ± 3	148 ± 3	148 ± 3	148 ± 3	164 ± 3	164 ± 3	30 ± 1	8 ± 0.4	54 ± 1	2 × 10 <sup>-9</sup>	2 × 10 <sup>-10</sup>	
SGS	5000	737 ± 5	1498 ± 19	141 ± 4	188 ± 3	188 ± 3	209 ± 4	209 ± 4	209 ± 4	40 ± 1	8 ± 0.4	54 ± 1	1 × 10 <sup>-9</sup>	2 × 10 <sup>-10</sup>	

#### **F.4 Additional results from the real data analysis**

Table A7: Variable screening metrics for SGS applied to real data in 5.2. The number of variables in  $\mathcal{A}_v$ ,  $\mathcal{S}_v$ ,  $\mathcal{E}_v$ , and  $\mathcal{K}_v$  are shown. The results are averaged across the nine pathway collections, with standard errors shown.

DATASET	METHOD	INPUT DIM	card( $\mathcal{A}_v$ )	card( $\mathcal{S}_v$ )	card( $\mathcal{E}_v$ )	card( $\mathcal{K}_v$ )
SGS	CANCER	5651	71 ± 1	211 ± 4	212 ± 4	1 ± 0.04
SGS	COLITIS	10259	25 ± 1	208 ± 6	209 ± 6	1 ± 0.07

Table A8: General and group screening metrics for SGS and gSLOPE applied to real data in 5.2. General metrics: the runtime (in seconds) for screening against no screening, the number of fitting iterations for screening against no screening (with the number of occasions of failed convergence given in brackets), and the  $\ell_2$  distance between the fitted values obtained with screening and no screening. Group screening metrics: the number of groups in  $\mathcal{A}_g$ ,  $\mathcal{S}_g$ ,  $\mathcal{E}_g$ , and  $\mathcal{K}_g$ . The results are averaged across the nine pathway collections, with standard errors shown.

METHOD	DATASET	INPUT DIM	card( $\mathcal{A}_g$ )	card( $\mathcal{S}_g$ )	card( $\mathcal{E}_g$ )	card( $\mathcal{K}_g$ )	NUM IT SCREEN (NUM FAILED)	NUM IT NO SCREEN (NUM FAILED)	$\ell_2$ DIST TO NO SCREEN
GSLOPE	CANCER	592	66 ± 1	120 ± 2	120 ± 2	0 ± 0	1719 ± 63(16)	4453 ± 103(186)	$7 \times 10^{-8} \pm 7 \times 10^{-9}$
GSLOPE	COLITIS	655	32 ± 1	56 ± 2	56 ± 2	0 ± 0	1215 ± 73(28)	3904 ± 127(140)	$3 \times 10^{-7} \pm 5 \times 10^{-8}$
SGS	CANCER	592	50 ± 1	167 ± 2	115 ± 2	67 ± 0.8	72 ± 3(0)	127 ± 4(0)	$1 \times 10^{-8} \pm 1 \times 8^{-10}$
SGS	COLITIS	655	18 ± 0.6	136 ± 4	87 ± 3	61 ± 2	156 ± 9(0)	1348 ± 62(0)	$4 \times 10^{-8} \pm 6 \times 10^{-9}$